Vivianite scaling in wastewater treatment plants

Occurrence, formation mechanisms and mitigation solutions

Prot, T.; Korving, L.; Dugulan, A. I.; Goubitz, K.; van Loosdrecht, M. C.M.

Important note
To cite this publication, please use the final published version (if applicable).
Please check the document version above.

Vivianite scaling in wastewater treatment plants: Occurrence, formation mechanisms and mitigation solutions

T. Prot [a,b,*], L. Korving [a], A.I. Dugulan [c], K. Goubitz [c], M.C.M. van Loosdrecht [b]

[a] *Wetsus, European Centre Of Excellence for Sustainable Water Technology, Oostergoweg 9, 8911 MA, Leeuwarden, Netherlands*
[b] *Dept. Biotechnology, Delft University of Technology, Van der Maasweg 9, 2629 HZ Delft, Netherlands*
[c] *Fundamental Aspects Mat & Energy Group, Delft University of Technology, Mekelweg 15, 2629 JB Delft, Netherlands*

ARTICLE INFO

ABSTRACT

The presence of soluble iron and phosphorus in wastewater sludge can lead to vivianite scaling. This problem is not often reported in literature, most likely due to the difficult identification and quantification of this mineral. It is usually present as a hard and blue deposit that can also be brown or black depending on its composition and location. From samples and information gathered in 14 wastewater treatment plants worldwide, it became clear that vivianite scaling is common and can cause operational issues. Vivianite scaling mainly occurred in 3 zones, for which formation hypotheses were discussed. Firstly, iron reduction seems to be the trigger for scaling in anaerobic zones like sludge pipes, mainly after sludge thickening. Secondly, pH increase was evaluated to be the major cause for the formation of a mixed scaling (a majority of oxidized vivianite with some iron hydroxides) around dewatering centrifuges of undigested sludge. Thirdly, the temperature dependence of vivianite solubility appears to be the driver for vivianite deposition in heat exchanger around mesophilic digesters (37 °C), while higher temperatures potentially aggravate the phenomenon, for instance in thermophilic digesters. Mitigation solutions like the use of buffer tanks or steam injections are discussed. Finally, best practices for safe mixing of sludges with each other are proposed, since poor admixing can contribute to scaling aggravation. The relevance of this study lays in the occurrence of ironphosphate scaling, while the use of iron coagulants will probably increase in the future to meet more stringent phosphorus discharge limits.

1. Introduction

Wastewater treatment greatly developed in the last decades. In 2014, about 95% of the European population (EU 28) was connected to a wastewater collection system, which accounts for around 517 million people (European commission 2017). Additionally, nutrient removal is practiced in 84.5% of the wastewater treatment plants (WWTP) through tertiary treatment (European commission 2017). The current direction is to evolve from the standard wastewater treatment practise towards a Water Resource Recovery Facility (Solon et al., 2019). Specifically, sludge is increasingly used to produce biogas, while phosphorus can be recovered, for example, as struvite ($NH_4MgPO_4 \times 6H_2O$) in installations where phosphorus is removed biologically (Partlan 2018).

Originally, the interest in struvite was not based on its recovery, but on the prevention of its presence as scaling. The occur-

rence of struvite scaling in WWTPs is long time recognised in literature (Rawn et al., 1939; Doyle et al., 2002) and is a plague. It can cause pipe diameter reduction, thus increasing the required pumping energy and eventually pipe replacement amongst other problems (Doyle and Parsons, 2002). Struvite scaling is predominantly reported in the dewatering units after digestion in WWTPs using Enhanced Biological Phosphorus Removal (EBPR), as phosphorus is released and solubilized during sludge digestion.

Another phosphorus mineral, vivianite ($Fe_3(PO_4)_2 \times 8H_2O$), can also cause scaling problems in WWTPs. It provokes the same operational problems as described for struvite and can involve important maintenance costs. Vivianite recently received increased attention since it was recognised as the major phosphorus mineral in iron-coagulated digested sludge (Wilfert et al., 2016), and could be recovered by magnetic separation (Prot et al., 2019). Due to its quick oxidation after exposure to air and light, vivianite scaling usually presents a blueish colour, facilitating an easy identification (Čermáková et al., 2013; McCammon and Burns, 1980). Nonetheless, we believe that vivianite scaling is not always identified due

to the general lack of information about its occurrence. Moreover, it is often misattributed to struvite scaling, which explains why vivianite scaling received little attention in the past. Twenty years ago, WWTP professionals started to report vivianite scaling in their installations (Marx et al., 2001; Shimada et al., 2011; Bjorn 2010), but this type of scaling was never studied in depth.

The understanding and prevention of vivianite scaling is a relevant topic due to the current lack of information, and to the expected increased use of iron salts in the future. Indeed, Chemical Phosphorus Removal (CPR) or a combination of CPR and EBPR can achieve lower phosphorus levels in the effluent than EBPR alone (El-Bestawy et al., 2005; Kumar et al., 2018). Additionally, precipitation is proposed as effective way to make WWTP's energy neutral or energy producing. Therefore, the number of WWTPs relying on (partial) CPR strategy is expected to increase, as it is already the case in North-West Europe (ESPP 2019), to comply to more stringent legislations for the effluent quality. Furthermore, high iron dosages are essential to maximize the amount of phosphorus that is recoverable magnetically (Prot et al., 2020), and it is important to ensure that it is compatible with vivianite scaling prevention. It is possible that vivianite scaling is already widely occurring nowadays, but without being identified. Vivianite identification is challenging without advanced techniques like Mössbauer spectroscopy since it can be highly oxidized and therefore become amorphous (Prot et al., 2020).

We reviewed the information available in literature for cases of WWTPs experiencing vivianite scaling. Since the data on vivianite scaling was limited in literature, information was also gathered from WWTPs suffering from vivianite scaling. In total, data from 14 WWTPs worldwide were collected to get a better overview of the situation. After identifying the preferential places for scaling, thorough analyses of a number of scaling samples were carried out. The possible formation mechanisms were discussed to finally evaluate several scaling mitigation strategies.

2. Materials & methods

2.1. WWTPs studied

In total, information from 14 WWTPs has been gathered, some of them presenting several places where scaling was observed. Fig. A1 depicts the location of these WWTPs and the type of information gathered.

2.2. Analyses

The scaling samples were not protected from oxygen and were stored for up to 6 months before analysis. Visual observations suggested that the centre of the samples was relatively protected from oxidation since it kept the same colour even after 6 months of storage, while vivianite oxidation is characterized by darkening of the samples from light to dark blue (Čermáková et al., 2013; McCammon and Burns, 1980). However, it cannot be completely excluded that the samples partly oxidized during their storage before the measurements. The samples were analysed to determine their elemental composition and their phase composition. In addition, pH, iron and phosphorus measurements were carried out in the sludge line of the WWTP of Hoensbroek (NL) of Waterschapbedrijf Limburg, using Hach-Lange kits. Chemical equilibrium modelling was conducted with the software Visual Minteq: the equilibrium reactions considered are detailed in Appendix B.

2.2.1. Elemental composition

At first, 30–50 mg of powdered sample was added to 10 mL of ultrapure HNO_3 (64.5 – 70.5% from VWR Chemicals) in a Teflon vessel. The powder was then digested in an Ethos Easy digester

from Milestone equipped with an SK-15 High-Pressure Rotor. The digester reached 200 °C in 15 min, ran at this temperature for 15 min, and cooled down for 1 h.

The elemental composition of the digestates was determined via Inductively Coupled Plasma (Perkin Elmer, type Optima 5300 DV) equipped with an Optical Emission Spectroscopy (ICP-OES). An Autosampler, Perkin Elmer, type ESI-SC-4 DX fast was used, and the data were processed with the software Perkin Elmer WinLab32. The rinse and internal standard solution were respectively 2% of HNO_3 and 10 mg/L of Yttrium.

2.2.2. Solid characterization

Firstly, a thin slice of each sample was cut with a scalpel for light microscope and SEM-EDX observation. The microscope used was a Leica MZ95 equipped with a Leica DFC320 camera. The SEM-EDX apparatus was a JEOL JSM-6480 LV Scanning Electron Microscope (SEM) equipped with an Oxford Instruments x-act SDD Energy Dispersive X-ray (EDX) spectrometer. The accelerating voltage was 15.00 kV for a working distance of 10 mm. The samples were covered with a 10 nm-layer of gold using a JEOL JFC-1200 fine coater to make the surface electrically conductive. The software used was JEOL SEM Control User Interface for the SEM and Oxford Instruments Aztec for the EDX data processing.

Then, the samples were pulverized in a mortar for XRD, Mössbauer spectroscopy and carbonate analysis. Due to organization changes in TU Delft, 2 XRD devices were used. The first one was a PANalytical X́Pert PRO diffractometer with Cu-Kα radiation (5–80°2θ, step size 0.008°). The peaks assignment was realized with the software Origin Pro 9 (samples measured with this device: Venlo, Hoensbroek). The second device was a Bruker D8 Advance diffractometer Bragg-Brentano geometry and Lynxeye position sensitive detector with Cu-Kα radiation (10–80°2θ, step size 0.008°). The peaks assignment was done with Bruker software DiffracSuite.EVA vs 5.2 (Samples measured with the second device: Spokane County, Amsterdam, Blue Plains, Turku).

In addition, Mössbauer spectroscopy was performed on a selection of samples to study the iron compounds, even those with an amorphous nature, which is not possible with XRD alone. The powdered samples were first introduced in plastic rings sealed with Kapton foil and Epoxy glue and wrapped in aluminium foil. If necessary, carbon powder was added to the sample to maintain a maximum iron quantity of 17.5 mg of Fe/cm^2. Transmission ^{57}Fe Mössbauer absorption spectra were collected at 300 K with conventional constant-acceleration spectrometer using a ^{57}Co (Rh) source. One sample (from Turku) was also analysed at 4.2 K for further analysis of the Fe(III) phases. Velocity calibration was carried out using an α-Fe foil. The Mössbauer spectra were fitted using the Mosswinn 4.0 program (Klencsár 1997) and based on previous fittings of sludge samples as described in Wilfert et al., 2018 and Prot et al., 2020.

Literature data on vivianite scaling are scarce and not detailed enough to understand the scaling formation mechanisms. Therefore, 10 WWTPs experiencing vivianite scaling were directly contacted to gather additional information and samples (Table 1). The collection of these data allowed the identification of the preferential vivianite scaling zones. The possible formation mechanisms were then proposed and correlated to the composition of the vivianite scaling samples. When necessary, more detailed analysis was carried out at the WWTPs to challenge the proposed formation mechanisms.

3. Results & discussion

From the data collected at 14 WWTP's (Fig. A1), five possible locations for vivianite scaling formation in a WWTP were identified. These locations are discussed in the following sections: in the

Table 1

Inventory of the vivianite scaling observed by the WWTPs contacted during this study, as well as previously reported in literature.

Hot-spot	WWTP	Zone description	Source	Composition (mg/g)					Phase identification			CO$_3$ (%)
				Fe	P	Mg	Ca	S	XRD	Mössbauer	Light microscope/SEM-EDX	
Sludge transport or handling units under anaerobic conditions	Hoensbroek	Pipe after the thickener	This study	309	95	4		41	Vivianite	72% vivianite Possible FeS mineral	Blue zone with Fe/P overlay Orange zone with Fe/S overlay	0.1 ± 0.1
	Dokhaven	Sludge buffer tank for B-stage	This study	319	123	4	8	2	nd	nd	Blue crystals with the same structure as vivianite	0.0 ± 0.1
	Venlo	Pipe after the thickener	Prot et al., 2019	308	119	11	10	2	Vivianite	68% vivianite	Layered blue scaling Homogeneous elemental distribution	nd
	Bosscherveld	Pipe after the thickener	This study	191	98	3	47	3	nd	nd	Blue crystal with the same structure as vivianite	0.0 ± 0.1
	Blue Plains	In equipment pre-centrifuge	Pathak et al., 2018	nd					Vivianite	nd	nd	nd
Pre-dewatering centrifuge	Hoensbroek	Centrifuge tank and subsequent centrate pipe	This study	259	112	2	44	2	Vivianite	23% vivianite	Major brown phase Minor blue phase Homogeneous elemental distribution	0.2 ± 0.1
	Turku		This study	393	41	1	14	2	Major amorphous phase Minor goethite	70% Ferryhydrite 30% santabarbaraite	Brown amorphous phase More crystalline black phase Homo. elemental distribution	0.5 ± 0.1
	Bosscherveld		This study	282	107	6	9	2	nd	nd	Layered black, brown, light-brown scaling with a blue layer on the inside	0.2 ± 0.1
	Blue Plains		This study	307	109	2	23	1	nd	nd	Major brown phase Minor blue phase Homogeneous elemental distribution	0.3 ± 0.1
			Pathak et al., 2018	nd					Minor vivianite Major amorphous phase	nd	nd	nd

Table 1 (*continued*)

Hot-spot	WWTP	Zone description	Source	Composition (mg/g)					Phase identification			CO$_3$ (%)
				Fe	P	Mg	Ca	S	XRD	Mössbauer	Light microscope/SEM-EDX	
Heat exchangers (HE)	Amsterdam	HE around the mesophilic digester	This study	298	129	18	11	3	Baricite (impure vivianite) Quartz, low	68% vivianite	Layered blue scaling Homogeneous elemental distribution	0.0 ± 0.1
	Dallas		Shimada et al., 2011	122	23	6	7	nd	Vivianite (method not mentioned)			nd
	Lübeck		Contact with the WWTP	nd					Vivianite (visual observation and laboratory analysis)			nd
	Ejby Mølle		Contact with the WWTP	nd					Vivianite (XRD)			nd
	Back's river		Marx et al., 2001	nd					Vivianite (method not mentioned)			nd
	Derby	HE around the mesophilic APD	Bjorn 2010	nd					Vivianite (method not mentioned)			nd
	Nine Springs	HE around thermophilic digestion	Reusser 2009	nd					Vivianite (method not mentioned)			nd
	Blue Plains	Cooling HE after THP	This study	319	118	10	3	8	Baricite (impure vivianite)	72% of vivianite	Blue zone with Fe/P overlay Orange zone with Fe/S overlay	0.3 ± 0.1
	Venlo	Cooling HE after THP	This study	87	113	26	98	11	nd	nd	Homogeneous black layer (amorphous) Homogeneous elemental distribution	0.0 ± 0.1
Digester	Spokane County	Digester withdrawal	This study	310	87	3	20	1	Vivianite Rhodochrosite (possible siderite)	45% vivianite 11% possibly siderite	Dark blue particles (microscopic structure of vivianite) Quartz like transparent particles Orange particles	4.8 ± 0.3
	Blue Plains	Digester withdrawal	This study	89	29	5	9	3	nd	nd	Vivianite-like dark blue particles Quartz like transparent particles	nd

nd: no data means that the information was not available in the literature reference, or that we did not analyse the sample with this method.
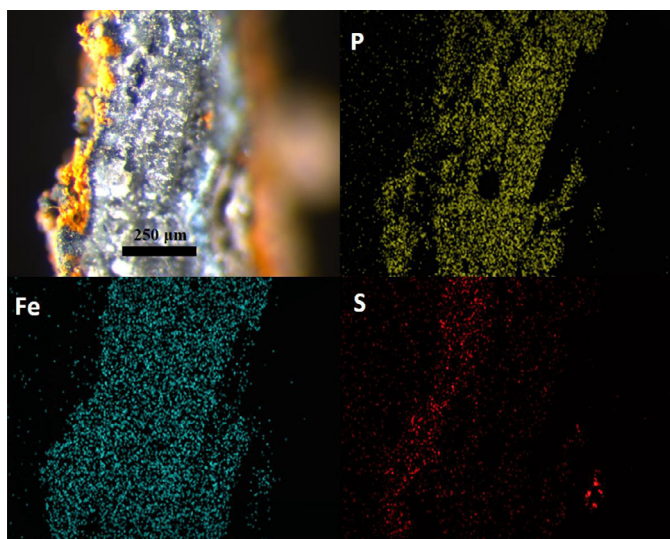
Fig. 1. Light microscope picture of the scaling in the anaerobic pipe of Hoensbroek (top left). Corresponding elemental distribution by EDX for Phosphorus (top right), iron (bottom left) and sulphur (bottom right). The blue phase of the microscope picture is vivianite (Fe and P overlap) while the orange phase is a FeS mineral (Fe and S overlap).

anaerobic pipes and units before sludge digestion (3.1), around the dewatering centrifuges for undigested sludge (3.2), in the heat exchangers around anaerobic digestion (3.3), in zones where sludge with different characteristics are mixed together (3.4), and in digesters as settled particles (3.5). The possible mechanisms of formation of vivianite scaling are discussed resulting in a proposal for strategies to prevent vivianite related scaling.

3.1. Anaerobic zones

Our dataset indicates that one preferential place for vivianite scaling are pipes and storage tanks for waste sludge, where sludge is maintained under anaerobic conditions for several hours. In the WWTP of Blue Plains, scaling was observed in several units downstream of the sludge thickener (screens, flow meters, valves, centrifuge feed). The WWTP of Venlo also experiences scaling before the Thermal Hydrolysis Process (THP) installation, mainly in the pipes and sludge cutter after the thickener. At the WWTPs of Hoensbroek and Bosscherveld, a blueish scaling was observed in the pipes carrying the sludge from the thickener to the dewatering centrifuge. This scaling provoked operational issues, forcing the shut-down of centrifuges for cleaning, while restricting the flow in the pipeline (Pathak et al., 2018).

XRD indicated that no other crystalline phases than vivianite were present in Hoensbroek and Venlo, while some quartz and siderite were also found in Blue Plains in 2 out of 6 samples (Pathak et al., 2018). While XRD is limited to the analysis of the crystalline phases, Mössbauer spectroscopy allows to also quantify any amorphous Fe-compounds. Mössbauer spectroscopy revealed that vivianite was accounting for 72% and 82% of the total weight of the scaling in Hoensbroek and Venlo, respectively. The unidentified part of the scaling could be other iron species like Fe(III) phases or a low-spin Fe(II) phase (typically FeS minerals) according to Mössbauer spectroscopy. These species could be iron oxides resulting from the ageing of vivianite (Roldan et al. 2002). In the case of Hoensbroek, the 4% of sulphur exactly accounts for the iron fraction not bound to vivianite if formation of FeS is assumed, which is also in line with EDX results (Fig. 1). The vivianite present in the scaling can be impure and also include Mg and Ca in its structure as noticed by Rothe et al., 2016 and Seitz et al., 1973. Therefore,

we hypothesize that the scaling was actually composed of more than 72% (Hoensbroek) and 82% (Venlo) (value obtained assuming no iron substitution) of a vivianite-like mineral.

Even though the different scalings do not have the exact same composition, we believe that the cause of their formation is identical. The scaling could result of the formation of stable nuclei on the surface on a surface (e.g. wall of a pipe) through primary heterogeneous nucleation, being the onset for further crystal (in this case scaling) growth (Mersmann 2001). Alternatively, agglomeration could be triggered by deposition of small vivianite crystals (resulting from previous nucleation) on the surface of the equipment or pipe. Turbulence in the pipe or equipment near the walls increases collision probabilities and forms an important factor for this mechanism (Mersmann 2001). Fluid mechanics in the pipe system have been studied to discuss this point. The main findings are presented in this section, while the detailed calculation can be found in Appendix C. In Hoensbroek, the activated sludge is brought to a thickener with a residence time of 13 h, before being pumped toward a centrifuge at a flow of 18.7 m^3/h via three consecutive pipes (d_1=0.2 m/l_1=30 m; d_2=0.1 m/l_2=5 m; d_3=0.08 m/l_3=16 m). Considering a power-law model approach, the flow regime is laminar in pipe 3 since Re<2100 (Ratkovich et al., 2013), so the flow is also laminar in pipe 1 and 2 since they have bigger diameters. This is in line with what is reported in literature, where sludge flow in pipes is usually considered laminar (Slatter 2004; Haldenwang et al., 2012). A collision formation mechanism seems unlikely in a laminar regime since it would require some transversal vivianite particle movement. Moreover, light microscope/SEM observations of the sample from Hoensbroek and Venlo show continuous crystalline matrix rather than agglomeration of particles, indicating that a growth mechanism from soluble phosphorus and Fe^{2+} is more likely (Fig. 1).

Since between the thickener and the dewatering units the conditions are anaerobic, Fe(III) will be reduced to Fe(II), while phosphate could be released from the biomass. According to rate measurements by Wang et al., 2019, it takes around 1 day to reduce the majority of the Fe(III) present in activated sludge to Fe(II). Around 2 days are required to release the biggest fraction of the phosphate from the Phosphate Accumulating Organisms (PAO's) during thickening according to Janssen et al., 2002. Considering that the typical sludge retention time in a thickener is a few hours, the release of phosphorus and iron will still be ongoing while the sludge will leave the thickener, allowing scaling growth. In iron-coagulated sludge (like in Hoensbroek), phosphorus is not only found in PAO's, but also bound to iron. It is complicated to evaluate separately the phosphorus released from PAO's and from Fe(III)P minerals. The study of the vivianite scaling formation was realized assuming that iron is the limiting compound, since phosphorus release mechanisms are more complex.

According to Wang et al., 2019, iron reduction follows a first-order kinetic with $k = 0.05$ h^{-1}, so the quantity of iron reduced in the pipes is proportional to the sludge retention time for low retention times. From the sludge velocity profile in the pipes, the zone next to the pipe wall will present a much smaller velocity and so higher Fe^{2+} concentration than in the bulk. From this, we can assume that the formation of vivianite follows a wall-mechanism, rather than a bulk-mechanism. Bigger pipe will see more iron being reduced compared to smaller pipes, due to higher retention times. However, a big part of the Fe^{2+} produced will not have time to diffuse to the pipe wall and will precipitate in the bulk, not causing scaling (Appendix C).

To summarize, the morphology of the scaling, and the laminar flow regime suggest that the scaling found in the sludge transport or handling units under anaerobic conditions follows a growth mechanism rather than an agglomeration mechanism. We hypothesize that the iron reduction due to the anaerobic conditions is the
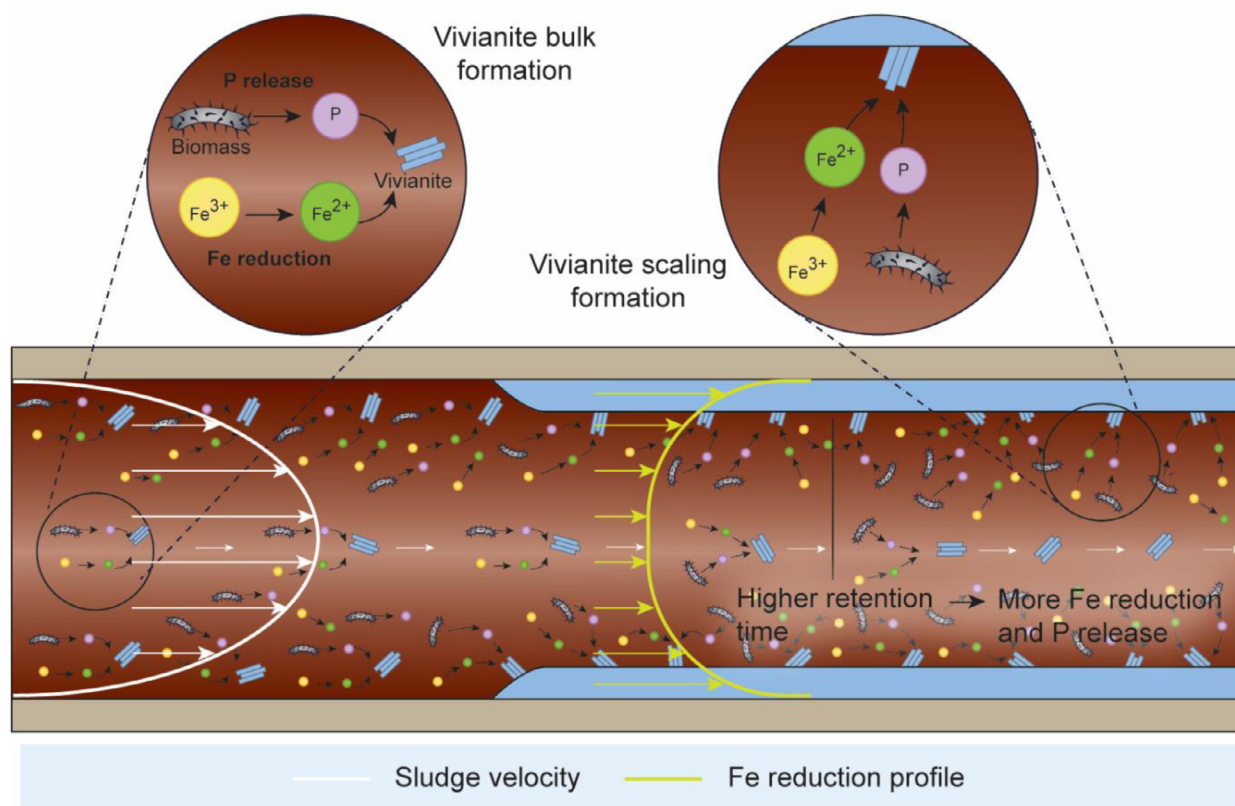
Fig. 2. Proposed formation mechanism of vivianite scaling in an anaerobic pipe. This figure highlights the difference between bulk and scaling formation, and the importance of the sludge velocity and iron reduction profile.

driver for the formation of the scaling (Fig. 2). Both low diffusion velocities and high iron concentrations near the walls suggest that a wall-mechanism growth is favoured. These observations imply that larger diameter pipes may be better to use due to their lower wall area/volume ratio, even though they present higher sludge retention times. Iron reduction and phosphorus release will strongly contribute to the formation of vivianite scaling and are unavoidable. However, iron reduction should be almost complete after 24 h according to Wang et al., 2019. This means that allowing a fermenting sludge to rest in a unit bearing a high volume/surface ratio (eg. a buffer tank) for a day could allow all the iron to be reduced and the main part of the vivianite to form in the bulk of the sludge, instead of creating problematic scaling in the units downstream. A small fraction of the vivianite could still scale on the wall of the buffer tank, but this should be manageable and is easily accessible for cleaning. Such buffer tank is used in the WWTP of Dokhaven (for a different purpose than scaling prevention). Vivianite scales were observed in this tank but it is not a major issue since it only requires a yearly cleaning. No scaling problem downstream from this tank has been reported, indicating that addition of such buffer tank may be a valid option for scaling prevention.

3.2. Dewatering units

From the information collected, the worst occurrence of scaling was around centrifuges used for the dewatering of undigested sludge. The WWTPs of Hoensbroek, Bosscherveld and Turku dewater their thickened sludge by centrifugation before sending it for disposal. The scaling occurs in Turku WWTP in the centrifuge and centrate pipe and is manageable with a manual cleaning being necessary 2–3 times per year, costing around 2000€/month (infor-

mation obtained from the WWTP). The situation is more dramatic in Hoensbroek and Bosscherveld where important build-up of scaling, mainly composed of vivianite-based compounds, was observed in the centrifuge, the centrate box and the centrate pipe. It forces a stoppage and cleaning of the centrifuge every 1–2 weeks and a yearly replacement of the centrate pipe in Hoensbroek. Scaling formation also happened in the WWTP of the Blue Plains in and downstream of the pre-dewatering centrifuge before THP. Build-up in the centrifuge increased torque and vibration, obliging operators to put the equipment out of service for manual cleaning (Pathak et al., 2018). Scaling formation in the centrifuge and the centrate pipes caused the most severe operational problems compared to the other scaling location.

Since the scaling observed in the centrifuges and in the centrate pipes are similar in their elemental composition and microscopic structures (unpublished data), detailed analyses were only carried out on the samples found in the centrate pipes. The samples were quite different from the scaling found in the heat exchangers and the sludge transport pipes since the deposits were softer and mainly brown/black instead of blue. The scaling from Blue Plains, Hoensbroek and Bosscherveld presented a similar elemental composition with 26–31% of Fe, 10–11% of P and 1–4% of Ca, which is close to the composition of vivianite (33% of Fe/12% of P) (Table 1). The samples were much more XRD-amorphous than the scaling found in other sections of the WWTPs, but XRD still managed to identify vivianite: impure in Hoensbroek, and as a minor fraction in Blue Plains (Pathak et al., 2018). Microscopic observations of these three samples revealed a structure with brown, black, and occasional blue layers suggesting a mix of species with vivianite not being the major compound (Fig. 3). Surprisingly, EDX showed a homogeneous distribution of iron and phosphorus across
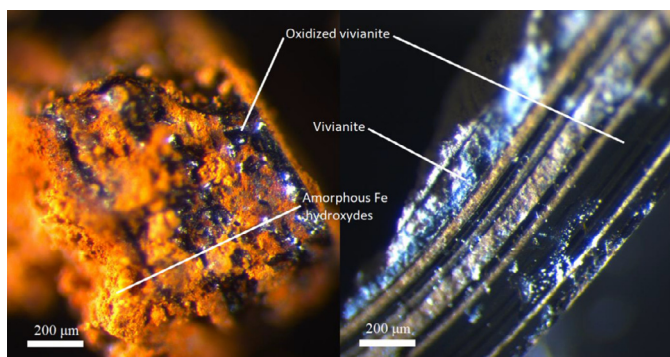
Fig. 3. Light microscope pictures of the scaling found in the centrate pipe of Turku (left) and Bosscherveld (right). Turku: slow formation mechanism dominated by ferrihydrite and a minor phase of fully oxidized vivianite (santabarbaraite). Bosscherveld: fast formation mechanism dominated by vivianite; a fresh vivianite layer can be observed on the sludge side while oxidized vivianite is present on the pipe side.

the samples. The Mössbauer spectroscopy study of the centrate sample from Hoensbroek confirmed the presence of 23% of vivianite, accounting for only 30% and 25% of the iron and phosphorus in the sample, respectively. The 70% of remaining iron is present in Fe(III) minerals according to Mössbauer spectroscopy. Based on the elemental composition close to the one of vivianite, we believe that vivianite originally formed and progressively oxidized (centrifuges are not protected from air intrusion), transforming into metavivianite ($Fe^{2+}Fe^{3+}_2(PO_4)_2(OH)_2 \cdot 6H_2O$) and then santabarbaraite (($Fe^{3+})_3(PO_4)_2(OH)_3 \cdot 5H_2O$). The structure of the scaling from Bosscherveld supports this hypothesis: it presents a blue layer (vivianite) on the most freshly formed side of the scaling, and brown/black Fe/P containing material (possibly metavivianite and santabarbaraite) deeper in the scaling (Fig. 3). Additionally, the EDX analyses revealed a homogeneous iron and phosphorus distribution across the entire sample. Oxidation of vivianite leads to the progressive destruction of its crystalline structure making the newly formed minerals undetectable by XRD (Dormann and Poullen, 1980; Pratesi et al., 2003). The Mössbauer signals of the oxidation products of vivianite are close to the one observed in this study (Fe^{III}: δ = 0.35–0.43 mm/s / QS = 0.5–0.9 mms/s according to Dormann and Poullen (1980), but are overlapping with the signal of iron oxides making it impossible to be attributed to metavivianite or santabarbaraite with certainty. Strengite is another possible Fe(III)P mineral, but the conditions in the centrifuge are not favourable for its formation (Wilfert et al., 2015; Pathak et al., 2018).

The sample from Turku is different in its composition (39% of Fe, 4% of P and 1% of Ca), appearance (major orange phase/minor black phase) and is really fragile (Fig. 3). Room temperature Mössbauer spectroscopy indicates that it is entirely composed by Fe(III) species (excluding the presence of vivianite and metavivianite) and contains ferrihydrite. Layered Iron hydroxide could be an intermediate since they are formed by oxidation of $Fe(OH)_2$ and inclusion of anions, and later form ferric oxyhydroxides under further oxidation (Refait et al., 1998). Phosphate adsorption alone cannot explain the 5% of phosphorus present in the sample since it would suggest a capacity 5 times higher (mg of P/g of Fe) than engineered Fe-adsorbents (Kumar et al., 2019). XRD indicated that the sample was mainly amorphous and could contain a small quantity of goethite, which agrees with Roldan et al. 2002, stating that vivianite oxidation results in the formation of poorly crystalline Fe(III) oxides, a polymorph of goethite. The 4.2 K Mössbauer spectroscopy measurement (which allows Fe(III) phases speciation) reveals that a mix of 23% santabarbaraite and 77% ferrihydrite is possible (Fig. 4 and Appendix H).
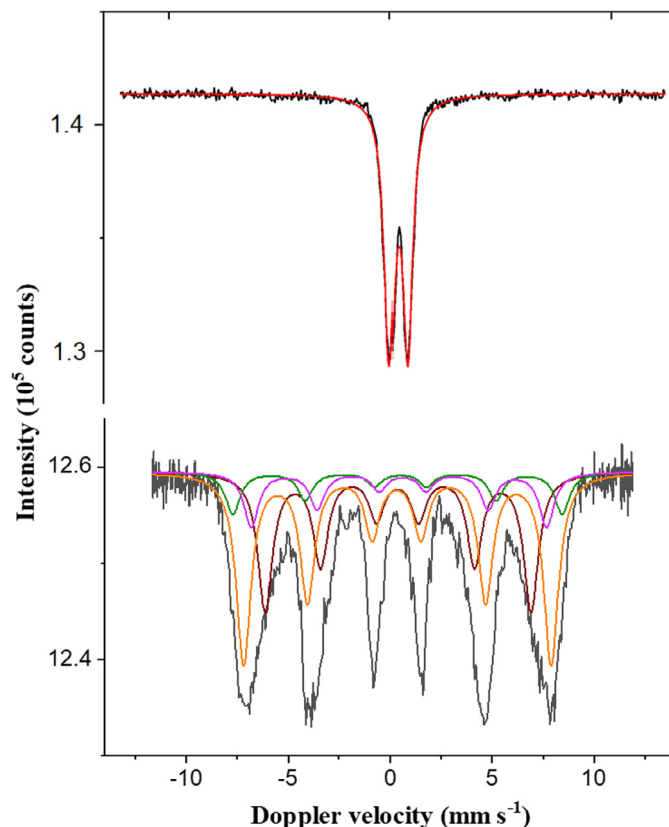
Fig. 4. Mössbauer spectra for the scaling in the centrate pipe of Turku at room temperature (top) and at 4.2 K (bottom). The top spectrum only reveals the presence of Fe^{3+} compounds without possible speciation (red curve). The bottom spectrum reveals the presence of fully oxidized vivianite (santabarbaraite) (green and pink curves) and of different ferrihydrite minerals with various degrees of crystallinity (orange and dark red curves). The fitting for low temperature measurement was based on experiments realized with oxidized synthetic vivianite (results not shown). More information is available in Appendix H.

The scalings found in centrate pipes are mainly amorphous and rich in phosphorus and oxidized Fe. The major compounds seems to be oxidation products of vivianite (metavivianite and santabarbaraite), while Fe(III) oxides/hydroxides are also present (except for Turku's sample where Fe(III) oxides/hydroxides are the main fraction). A pH increase favours both the precipitation of vivianite and iron oxides/hydroxide and could be the main mechanism explaining the formation of scaling around the centrifuge. Indeed, the pH increased by 0.3 during centrifugation in the WWTP of Blue Plains (Pathak et al., 2018) and Hoensbroek. The effect of pH on ferrihydrite precipitation is straightforward since its solubility directly depends on the third power of the OH^- activity (Schwertmann 1991). The SI of vivianite is proportional to the square of the activity of PO_4^{3-}, which is increasing with the pH (Liu et al., 2018). During centrifugation, CO_2 stripping occurs due to the turbulences and the contact with air, which triggers the observed pH increase (Battistoni et al., 1997). This rise of pH is also the main mechanism triggering struvite scaling in post-digestion dewatering centrifuges (Doyle and Parsons 2002). Taking into account the composition of the sludge liquor just before centrifugation in Hoensbroek (P = 8.6 ppm / Fe^{2+} = 27.4 ppm / Fe^{3+} = 6.91 ppm / pH = 6.9 / Ionic strength = 0.02), an increase to pH 7.22 signifies a SI increase from 5.41 to 6.28 and 5.48 to 5.80 for vivianite and ferrihydrite, respectively. The values of SI are high, which can be explained by an overestimation of $Fe^{2+/3+}$ in the sample. This overestimation is due to small colloidal iron particles going through the pores of the 0.45 μm-filter. We experimentally confirmed this but at a later mo-
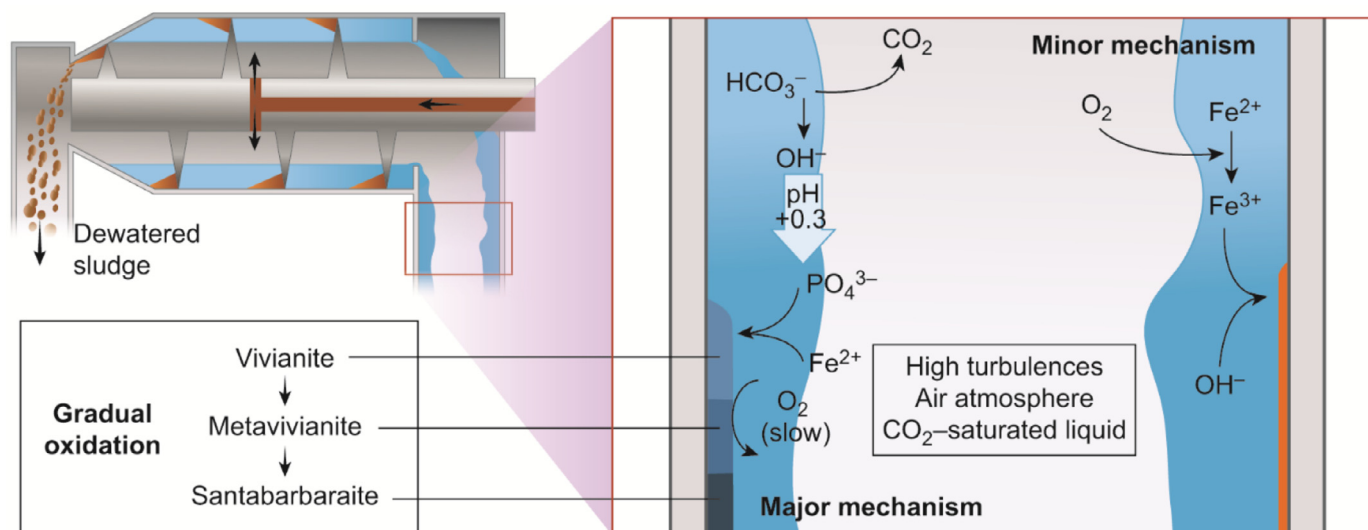
Fig. 5. Proposed formation mechanism of vivianite (major mechanism) and ferrihydrite (minor mechanism) in centrate pipes of pre-dewatering centrifuges. We assume that the formation mechanism is similar in the centrifuge itself. (vivianite: $Fe^{2+}_3(PO_4)_2 \cdot 8H_2O$, metavivianite: $Fe^{2+}Fe^{3+}_2(PO_4)_2(OH)_2 \cdot 6H_2O$, santabarbaraite: $(Fe^{3+})_3(PO_4)_2(OH)_3 \cdot 5H_2O$).

ment when the way of operation of the WWTP changed. Since iron reduction is a relatively slow process (compared to the instantaneous pH increase during centrifugation), we consider that a certain steady-state toward vivianite formation is established before centrifugation. The concentrations of iron and phosphorus were decreased assuming vivianite and $Fe(OH)_2$ formation to match the equilibrium SI calculated above (5.41 and 5.48). Such equilibrium conditions at pH = 7.22 are for P = 5.1 ppm / Fe^{2+} = 17.7 ppm / Fe^{3+} = 3.4 ppm, resulting in the formation of 28.3 mg/L of vivianite and 5.3 mg/L of ferrihydrite. It is clear that even a small pH increase can have an important effect on the precipitation of vivianite and ferrihydrite. From these calculations it appears that the scaling would be composed of a majority of vivianite, which reinforces our hypothesis that vivianite was initially formed, and oxidized, making it complicated to trace. A second mechanism could also explain the formation of Fe(III) oxides: since the centrifuge is not protected from air intrusion, the soluble Fe^{2+} could be oxidized, triggering the formation of poorly soluble $Fe(OH)_3$. Detailed calculations in Appendix D reveal that Fe(II) oxidation is too slow to explain significant formation of Fe(III) to produce $Fe(OH)_3$. It seems therefore that this mechanism is much less important compared to vivianite formation, which is confirmed by the information collected from the WWTPs: the centrate scaling from Hoensbroek, Blue Plains and Bosscherveld (containing a high quantity of Fe/P species) require regular cleaning, while the one in Turku (mainly iron oxide/hydroxide) only needs to be removed twice a year. The unique composition of Turku's sample may be explained by the high Fe/P molar ratio (1.75) used in this WWTP.

The reduction in the Fe^{2+} concentration in the liquid phase of the sludge to the centrate (27.4 to 6.5 ppm) is much larger when compared to the reduction in the phosphorus concentration (8.6 to 4.7 ppm) and cannot be explained by the formation of vivianite. The authors believe that this is due to an overestimation of the soluble iron before centrifugation as discussed above. Additionally, the extreme mixing conditions in the centrifuge may promote scaling formation. Indeed, the flow regime before the centrifuge is laminar, not allowing an optimal mixing of the ions, while centrifugation creates turbulent conditions. Yousuf and Frawley (2018) also showed that increased shear stress lowers the secondary nucleation (formation of crystals in the presence of parent crystals, Mersmann 2001) threshold by increasing the collision be-

tween particles. The presence of existing scaling and rough surface also promotes secondary nucleation.

From the information collected, it appears that scaling formation around centrifuges is mainly caused by a pH increase through CO_2 evolution in the centrate chamber and in a smaller extent by the oxidation of the soluble Fe^{2+} (Fig. 5). The large shear forces created by centrifugation can aggravate the scaling formation. Stripping some CO_2 in a tank before centrifugation to increase the pH would initiate controlled vivianite formation in the bulk and may reduce the scaling formation. Allowing a longer time under anaerobic conditions for the sludge before centrifugation should also lead to a reduction of soluble phosphorus and iron concentration. The addition of a buffer tank after the thickener could be a combined solution for the scaling around the centrifuge and in the anaerobic zones (discussed in 3.2). No vivianite scaling was reported in post-digester centrifuges, indicating that a longer residence time could indeed be a suitable solution. Since the pH increase is due to CO_2 stripping, creating a CO_2-saturated atmosphere in the centrifuge could theoretically be an option to prevent it. More research needs to be undertaken to evaluate the feasibility of all these options. Counterintuitively, a higher iron/phosphorus molar ratio in the sludge may also reduce vivianite scaling formation. A higher iron dosing reduces the quantity of phosphorus present in the soluble phase, reducing the quantity of phosphorus available for precipitation. Therefore, the pH increase observed during centrifugation would provoke less vivianite scaling formation. For example, the iron dosage in Turku is high (Fe/P = 1.75) and the scaling only needs to be removed 2–3 times per year. On the contrary, WWTPs dosing less iron (Fe/P = 1.14 in Hoensbroek and 0.65 in Bosscherveld) need to remove the scaling every 1–2 weeks.

3.3. Heat exchangers

From the information gathered from WWTPs, and supported by literature, it appears that sludge heat exchangers are a common place for vivianite scaling to occur. In the case of the WWTPs of Lübeck, Ejby Mølle and Amsterdam, a blue and hard scale was present in the sludge heat exchanger used for the heating of the mesophilic anaerobic digester. A similar situation was reported in literature in several other WWTPs: inside and downstream of the digested sludge heat exchanger in Dallas (Shimada et al.,
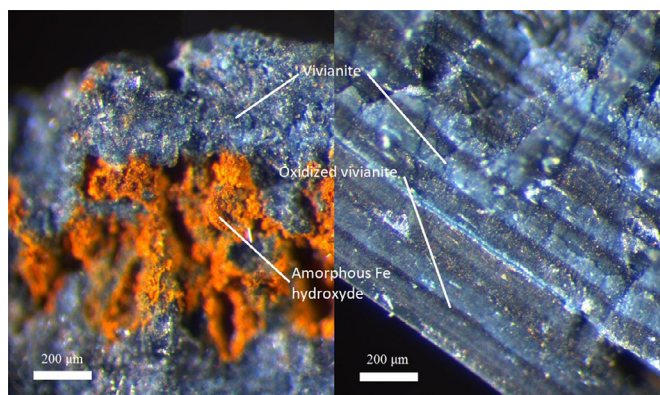
Fig. 6. Light microscope pictures of vivianite scaling found in the cooling heat exchanger after THP in Blue Plains WWTP (left) and in the heating heat exchanger around the mesophilic digester of Amsterdam (right).

2011), in the heat exchanger around the acid-phase digestion in Derby (Bjorn 2010) and in the heating loop in Back's River WWTP (Marx et al., 2001). Problems at higher temperatures, (especially in pasteurization units) have also been reported by Buchanan et al., 2014, Panter et al., 2013 and Reusser 2009. In the WWTP of Blue Plains and Venlo, scaling was found in the heat exchanger used to cool down the sludge after THP.

The seven scalings found in heat exchangers used to warm up the sludge for mesophilic and thermophilic digestion were all reported to be vivianite: by "laboratory analysis" in literature (not specified, but probably XRD and elemental analysis), by visual observation in Lübeck (no sample was available, only picture), and by XRD in Amsterdam and Ejby Mølle. The scaling of Amsterdam was further studied by Mössbauer spectroscopy, which confirmed the presence of vivianite as 68% in weight (likely underestimated due to its partial oxidation). The macroscopic and microscopic observations of the scaling from Amsterdam show a crystalline hard and blue scale that seems to be purer (no other phase than vivianite visually observed) than the scaling found in sludge pipes or dewatering units (Fig. 6). From the pictures available, the scalings from Lübeck and Ejby Mølle seem to have similar characteristics. This supposed high purity is supported by the elemental composition of the sample from Amsterdam: 30% of Fe, 13% of P and only 2% of Mg and 1% of Ca as inorganic impurities. It is interesting to note that Mg^{2+} and Ca^{2+} could be part of the structure of vivianite by substituting Fe^{2+} (Rothe et al., 2016; Seitz et al., 1973). The scale formed in the heat exchanger after THP at Blue Plains WWTP presents a similar elemental composition with 32% of Fe, 12% of P, 1% of Mg and 1% of S. However, this sample is more fragile, and composed of two main phases: a major blue phase, and an orange one (Fig. 6). Mössbauer spectroscopy results confirmed that the blue phase is vivianite, which accounts for 72% of the scaling weight (75% of the total Fe). The remaining 25% of iron are Fe(III) species according to Mössbauer spectroscopy, and could be a mix of iron oxides/hydroxides and metavivianite/santabarbaraite. The scaling found after THP in Venlo was black and had a completely different composition: 12% of P, 10% of Ca, 9% of Fe, 2.5 of Mg and 1% of S. No vivianite was present according to microscopic observations.

From the on-site observations described above, temperature seems to promote vivianite scaling formation both when the sludge is heated up, and cooled down. This is in line with the finding of Al-Borno and Tomson (1994) who showed that vivianite solubility evolves hyperbolically in function of the temperature (Fig. 7). Their results indicate that vivianite was the most soluble around 30–35 °C, which is close to the temperature of operation of a mesophilic digester (37 °C). The flow rate in heat exchanger is usually quite high (60 m^3/h for Amsterdam WWTP for example), which, together with their geometry (spiral shape, corrugated tubes…), promotes turbulences (Alfa Laval brochure 2020; Spiralex brochure, 2020) in order to prevent solid settling and thermal decomposition of organics (Lines 1991). If the flow is turbulent, a homogeneous temperature distribution can be expected in the bulk of the sludge. According to Guo (2020) only a very thin layer of sludge near the wall (the boundary-layer) will have a lower velocity (and so higher temperature) than the bulk, as opposed to the more gradual velocity gradient existing for laminar flows (Appendix C). The exact temperature of the wall has not been calculated since full description of the thermal situation was not the objective of this study.

From the information we collected, the digested sludge is brought typically from 30 °C to 38 °C by a water stream decreasing from 60 to 55 °C. According to Fig. 7, the solubility product constant (pK_{sp}) of vivianite slightly increases from 35.738 to 35.766 between 30 °C and 38 °C. It translates into the precipitation of a maximum 0.28 mg of vivianite per litre of sludge for a typical iron-coagulated digested sludge considered in Appendix E (P = 30 ppm, Fe^{2+}=15 ppm, IS=0.05, pH=7). Considering the flowrate of the sludge in the heat exchanger of Amsterdam WWTP (60 m^3/h), it corresponds to the precipitation of 16.8 g of vivianite per hour in one heat exchanger. It seems unrealistic that all the vivianite formed in the heat exchanger would scale, so this value is likely overestimated. It is important to mention that iron was dosed in the sludge heating loop of the WWTP of Amsterdam, which surely contributed to scaling formation. Even though the turbulent flow regime suggests a bulk mechanism, it is interesting to study what can happen in the boundary-layer of a heat exchanger. At the exit of the considered counter-current heat exchanger the temperature of the water is 60 °C, while the temperature of the sludge is 38 °C. Assuming that the wall temperature is the average of the temperature of the sludge and the heating water, 8 times more vivianite (2.17 g/L of sludge) could potentially form at the wall at 50 °C compared to the bulk at 38 °C. In Derby WWTP, peaks to 85 °C of the heating water where observed (and believed to aggravate the scaling), which would lead to potential formation of 4.96 mg/L of vivianite (considering a wall temperature of 60 °C). Fig. 7 suggests that vivianite is more likely to form in the exit part of the heat exchanger where the sludge is the warmest, which was observed by Reusser 2009. The situation could be worse when the sludge is brought at higher temperature (55 °C). Heating up sludge from 30 °C to 55 °C potentially produces 12 times more vivianite (3.4 mg/L) compared to heating up from 30 °C to 38 °C. Temperatures higher than 55 °C cause severe vivianite scaling issues particularly in heat exchanger of pre-pasteurization plants (Panter et al., 2013) and of a specific thermophilic digester configuration (Reusser 2009).

Salehin et al., 2019 did not find vivianite presence in digested sludge after THP by XRD, and concluded that vivianite formation was hindered by THP, which suggests that vivianite scaling would not occur after THP. However, our Mössbauer spectroscopy measurements revealed that vivianite accounted for 18% of the total solids in the post-THP digested sludge of Blue Plains WWTP, showing the possibility for vivianite to form. In the Cambi installation of Blue Plains WWTP, sludge after THP is cooled down from 160 to 41 °C, first by pressure reduction from steam release followed by dilution with process water, and then with a heat exchanger. It can be hypothesized that the vivianite scaling observed was formed in the colder sections of the heat exchanger (with wall temperature <32 °C according to Fig. 7). Vivianite scaling in the cooling heat exchanger after THP could then occur in the cold sludge region, while the warmer region should be scale-free. In the case of Venlo WWTP, THP is followed by thermophilic digestion at 55 °C. It is unlikely that the sludge temperature decreases below 32 °C in the
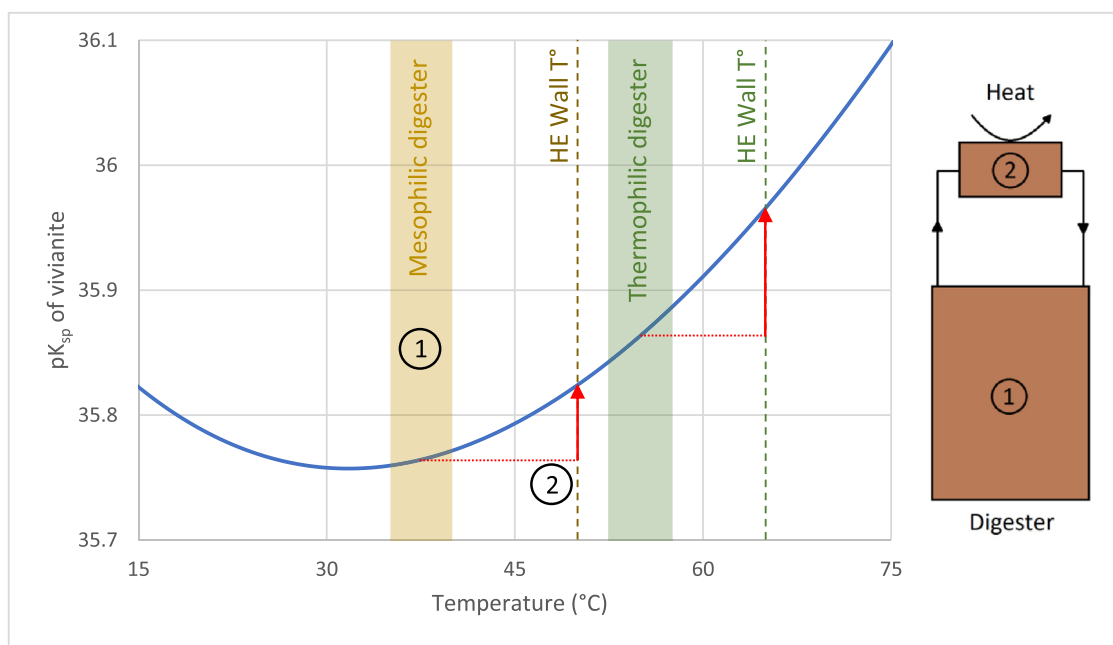
Fig. 7. Evolution of the negative logarithm (pK_{sp}) of vivianite in a function of the temperature. The figure was plotted following the relation obtained by Al Borno and Tomson 1994: $pKsp = -234.205 + 12{,}242.6/T + 92.510\, logT$, valid from 5 to 90 °C. The figure also shows the temperature range in mesophilic and thermophilic digester and the corresponding wall temperature of the corresponding heat exchanger (considering heating fluid temperature of 60 °C for mesophilic digester and 75 °C for thermophilic digester).

boundary-layer under these conditions, so it seems logical that no vivianite scaling was found there.

From the different hot-spots identified, vivianite scaling in the heat exchanger was the most commonly reported in literature (Table 1). It could be due to the fact that vivianite in heat exchangers is generally more recognisable ("clean" hard and blue scale), more accessible (compared to pipe inspection) and causing immediate operational issues (temperature losses as observed by Shimada et al., 2011 and Reusser 2009). While the scaling in the heat exchanger was manageable in most of the installations using mesophilic digestion, it seems that it can be more severe in installation bringing sludges at higher temperatures. Vivianite scaling was observed in both tubular and spiral heat exchanger Lübeck WWTP, so it is complicated to say which type of heat exchanger would cause less trouble. Using steam injection instead of contact heat exchangers to promote bulk precipitation is sometimes used and could be an interesting alternative to reduce scaling (Buchanan et al., 2014; Panter et al., 2013). However, it involves more energy and on-site production of boiled feed water, making this strategy more complicated to apply. In general, maintaining a low (and constant) temperature difference between the sludge and the heating water to avoid high wall temperature seems to be the best solution to mitigate vivianite scaling (Reusser 2009; Bjorn 2010), but is more complicated at thermophilic temperatures. Iron salt addition or sludge admixing (see 3.5) in the heat exchanger loop can aggravate the problems further.

3.4. Sludge admixing

An additional point that requires attention to control scaling formation is the way the different sludges are mixed together. Wastewater treatment produces different streams of sludge that will be brought together typically for pre-dewatering or digestion. Those sludges have different characteristics (pH, temperature, concentration of Fe^{2+} and PO_4^{3-}) and when they are brought together, the saturation index (SI) of the mix can potentially be higher than the index of the individual sludges. This can be particularly the

case when an already fermented sludge is mixed with a relatively fresh sludge. When a sludge ferments, pH drops (VFA production), Fe^{2+} increases (dissolution of iron precipitates), and PO_4^{3-} increases (poly-phosphate from PAO's hydrolysis). The difference of temperature between sludges can also be a factor triggering vivianite scaling. In Dallas WWTP, digester feed was periodically incorporated to recirculation sludge (Shimada et al., 2011), which can aggravate the problem due to an increase of the saturation index because of influences on composition (pH, Fe^{2+}, PO_4^{3-}) and temperature. Similar mixing issues, in addition to an increased pH due to CO_2 stripping were believed to aggravate vivianite scaling in Back River WWTP heating loop (Marx et al., 2001).

To conclude, mixing of different sludges can trigger or aggravate vivianite scaling. To prevent or at least mitigate vivianite scaling, it is important to minimize the pH, temperature and concentration differences between sludges that are mixed. This could be done by preferring continuous feed at a lower flowrate, over big periodical feed flows. More importantly, the place where the mixing occurs should be wisely chosen. The mixing of sludge should preferably happen in a unit where the volume to area ratio is high to favour bulk precipitation. The use of buffer tanks to allow the majority of the vivianite to precipitate seems ideal. On the contrary, we do not recommend to mix sludges in or before a unit where the surface/volume ratio is high (e.g. in the case of in-line mixing in pipes, heat exchanger, etc.).

3.5. Digester

Vivianite formation is promoted under anaerobic conditions due to the release of phosphate and the reduction of Fe(II), and anaerobic digesters are, therefore, a preferential formation site (Wilfert et al., 2018). Vivianite scaling could happen on the walls of digesters, similarly to struvite, but should not be so problematic due to the high volume/area ratio of digesters. The authors think that the settling of vivianite particles in digesters is not likely to happen since vivianite particles have the same density as quartz, but are usually smaller (100–150 μm maximum). We assume that
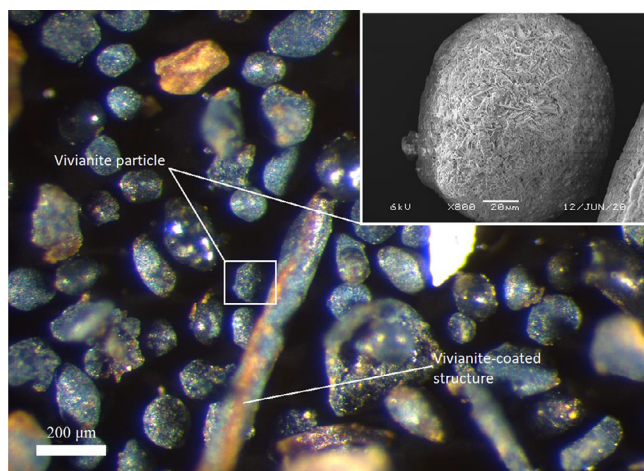
Fig. 8. Light microscope picture of the digester withdrawal obtained from Spokane County WWTP. EDX identified all the blue particles as vivianite and a SEM picture of one of those is shown on the top right. The problem in Spokane County digester originated from settling of free vivianite particles, and not deposition of a continuous vivianite scaling. (For interpretation of the references to colour in this figure legend, the reader is referred to the web version of this article.)

digester mixing is generally engineered in a way that it prevents settling of quartz and, similarly, settling of vivianite. Moreover, vivianite settling was never reported as an issue in any of the numerous digesters (bearing vivianite in their sludge) sampled by our team in previous studies (Wilfert et al., 2018). Blue Plains WWTP digester withdrawal contains some vivianite, but does not accumulate, not creating issues. However, the WWTP of Spokane County experiences problems in its anaerobic digesters due to the accumulation of a dark sand-like material, suspected to be vivianite (Fig. 8). Each digester is mixed with an external draft tube designed to pull from the centre of the bottom section and feed at the top, but that needs to be reversed when too much material has accumulated. Additional mixing is provided by an internal jet mixing ring located at the bottom of each digester. This jet mixing system has experienced clogging, potentially also caused by material accumulation. This accumulation obliges the WWTP to drain the bottom of the digesters on a daily-basis, losing a part of the valuable microbial community and involving heavy maintenance. On the contrary to previously discussed scaling problems, the issue in Spokane County digesters was the settling of vivianite particles, not the deposition of a continuous vivianite layer. This case was investigated to confirm the presence of vivianite, understand the cause of the settling, and evaluate the uniqueness of this situation.

The digester withdrawal is composed of a majority of Fe (32%) and P (9%), with 2% of Ca as the main other inorganic element. Mössbauer spectroscopy indicated that 45% of the sample is vivianite, and may contain non-detected oxidation products of vivianite (metavivianite and santabarbaraite) since 37% of the phosphorus is still not attributed. XRD detected the presence of baricite ((Mg, $Fe^{+2})_3(PO_4)_2 \cdot 8H_2O$) that can be assumed to be impure vivianite, and Rhodochrosite ($MnCO_3$). The later could in fact be siderite ($FeCO_3$) since Mn is absent from the sample and siderite has a similar XRD pattern as rhodochrosite (Anthony et al. 1990). Also, Mössbauer spectroscopy detects 11% of a Fe(II) phase with hyperfine parameters similar to siderite (Medina et al., 2006). The presence of siderite would also match with the 4.8% of CO_3 (equivalent to 9.6% of $FeCO_3$) detected by μGC (data not shown). The microscopic observations reveal that the majority of the sample was composed by blue particles presenting a Fe/P overlap (Fig. 8). These particles showed similar structure (sheets agglomerate) as the vivianite particles found in digested sludge (Wilfert et al., 2018;

Prot et al., 2019 and 2020), but were free and more spherical (a longer retention time in the digester could promote erosion). The particles were not bigger (100–150 μm) than the largest of the particles usually encountered in digested sludge.

The terminal settling velocity of a vivianite particle of 150 μm of diameter was evaluated to be 2.27 m/h (Appendix F). This velocity is smaller than the one produced by the digester mixing (vertical velocity ~20 m/h), so we would not expect the particles to settle. However, vivianite does settle, and the turnover time for these digesters is 1 h, which is in the high range compared to 4 digesters studied by Meroney and Colorado (2009) (24–54 min), suggesting a not sufficient mixing. From a discussion with the operators of the digesters of Spokane County, the mixing system is unique, and no other installations encountered similar settling problems. To conclude, the mixing design seems to be the major cause of the problem.

For the specific case of Spokane County WWTP, the addition of an alternative mixing system to the existing installation could provide sufficient mixing and appear to be the most efficient solution, but could be costly and complicated. The digester is emptied by an overflow at the top of the installation, which may not be optimal in this situation since the sludge is not homogeneous. Discharging from a lower point in the digester could help preventing vivianite accumulation. More generally, it is interesting to note that working at higher solid content in a digester would increase the viscosity of the sludge, and, therefore, lower the particle settling speed. For example, increasing the solid content from 2.5% (solid content in Spokane County WWTP) to 5% would decrease the settling velocity from 2.27 to 0.28 m/h (Appendix F). Lastly, we noticed that vivianite was agglomerating on some particles in the digester withdrawal, increasing their size, and therefore, their settling potential (Fig. 8). Accumulation of vivianite on sand particles (in a fluidized-bed reactor) was already proven possible by Priambodo et al., 2017. To avoid this agglomeration, solids, and especially sand should consistently be removed before digestion not to be used as a centre of agglomeration for vivianite.

3.6. Evaluation of the findings

From the information collected, it seems that vivianite scaling in WWTPs is occurring much more often than reported in literature. From the five preferential scaling places studied, three seems to be more common: 1. the anaerobic pipes and units before sludge digestion, 2. around the (pre-) dewatering centrifuges treating undigested sludge, and 3. in the heat exchangers around anaerobic digestion. Vivianite is usually the major component of the scaling in these three zones with FeS and iron oxides/hydroxides being minor phases. In the zone 2., vivianite gradually oxidizes to turn into amorphous metavivianite and santabarbaraite. The vivianite formation mechanism is different depending on the scaling place, and can involve iron reduction, pH increase or temperature changes. Different prevention solutions based on the formation mechanisms are proposed in

Table 2. A common prevention strategy is the use of commercial anti-scalant, which is not discussed in this study. It appears that the way sludge streams with different characteristics are admixed (e.g. raw sludge + digested sludge) is an aggravating factor of vivianite scaling. It should be done in unit with high volume/surface ratio like buffer tanks, to promote bulk precipitation. Vivianite settling in digesters cannot be classified as a common issue, since the case studied involved an unique mixing system, that we believe is the cause of the problem.

So far, vivianite scaling did not attract a lot of attention compared to struvite scaling since the importance of vivianite in wastewater treatment was only recently highlighted. Moreover, vivianite scaling is often wrongly mistaken for struvite scaling, while

Table 2

Summary of the preferential scaling places, the composition of the scaling, their proposed formation mechanisms and possible prevention methods.

Place where scaling occurs	Composition of the scaling	Formation mechanisms	Prevention methods
Anaerobic zones	Crystalline vivianite FeS (minor)	Fe(III) reduction coupled with phosphate release from biomass	Addition of a buffer tank to promote bulk precipitation before pumping the sludge. Prefer the use of large pipes
Dewatering units (for undigested sludge)	Vivianite (minor)	Turbulences leads to CO_2 stripping, which increases the pH.	Addition of a buffer tank to promote bulk precipitation before centrifugation.
	Metavivianite and santabarbaraite (major)	Gradual oxidation of vivianite	Centrifuging in CO_2-saturated atmosphere
	Fe oxides/hydroxides (generally minor)	Fe^{2+} oxidation (Fe^{3+} has a low solubility)	Centrifuging in O_2-free atmosphere (complicated)
Heat exchangers	Crystalline vivianite (few other compounds)	The solubility of vivianite varies with temperature.	Minimize the temperature between the heating/cooling fluid and the sludge.
	Fe oxides/hydroxides after THP only (minor)	Wall temperature are higher than the bulk	Steam injection for severe cases

the presence of struvite scaling was never detected in this study. It needs to be noted that struvite scaling is more likely to happen in WWTPs using EBPR (Parsons and Doyle 2002) while vivianite scaling should preferentially happen in WWTPs dosing iron to remove phosphorus. The absence of struvite scaling in the presence of iron can be explained by its lower solubility (6.31×10^{-5} M for $pK_{sp} = 12.6$) than the one of vivianite (6.92×10^{-8} M for $pK_{sp} = 35.8$). Also, vivianite oxidation leads to the formation of amorphous compounds that are more complicated to identify. Even Mössbauer spectroscopy analysis, the best option for vivianite quantification, presents limitations, especially due to an incomplete database on iron compounds in sludge. Iron addition may be favourable for energy production via enhanced primary settling, and we discussed in Prot et al., 2020 that higher iron dosage is favourable for vivianite formation and thus, for subsequent magnetic recovery. We foresee that higher iron dosing will be more commonly applied in the near future for different reasons: struvite scaling prevention, sulphide control in biogas and to meet more stringent legislation requirement for phosphorus removal. Additionally, higher iron dosing increases the share of phosphorus present as vivianite, which can subsequently be recovered via magnetic extraction, providing a new possible phosphorus recovery route (Prot et al., 2019, 2020). Dosing more iron is not incompatible with vivianite scaling prevention since bigger quantities of iron dosed achieve lower soluble phosphorus, more phosphorus chemically fixed, thus less phosphate released from biomass, reducing the phosphorus pool available for vivianite scaling. Vivianite scaling occurrence does not mean that the quantity of iron dosed needs to be adjusted, but rather that it needs to be dosed better. This study raises points of attention and proposes mitigation/prevention solutions that should be evaluated in each specific case by the water utilities.

4. Conclusion

The main conclusion of this study is that vivianite scaling is occurring more often than the lack of information in literature suggests. Three preferential scaling places could be identified, each of them presenting a different vivianite formation mechanism. Firstly, the reduction of ferric iron triggered the formation of crystalline vivianite in the sections where undigested sludge met anaerobic conditions (eg. thickened sludge pipes). Secondly, CO_2 stripping occurring during centrifugation of undigested sludge caused a pH increase, responsible for the formation of vivianite that could later oxidize to santabarbaraite. Thirdly, the temperature dependence of the solubility of vivianite can drive the formation of vivianite scaling on the walls of the heat exchangers used for digested sludge heating. Additionally, scaling prevention solutions were discussed in each case. For example, the use of an anaerobic buffer tank immediately after thickening would promote the formation of vivianite in the bulk of the sludge, reducing the vivianite scaling issues in the pipes and centrifuges downstream. The choice of the appropriate solution and the related cost analysis should be undertaken in each specific case since costs for maintenance and material vary depending on the WWTP design and location. We believe that this work can be of interest for water authorities for vivianite scaling mitigation, as well as for researchers investigating vivianite recovery from sewage sludge.

Declaration of Competing Interest

The authors declare that they have no known competing financial interests or personal relationships that could have appeared to influence the work reported in this paper.
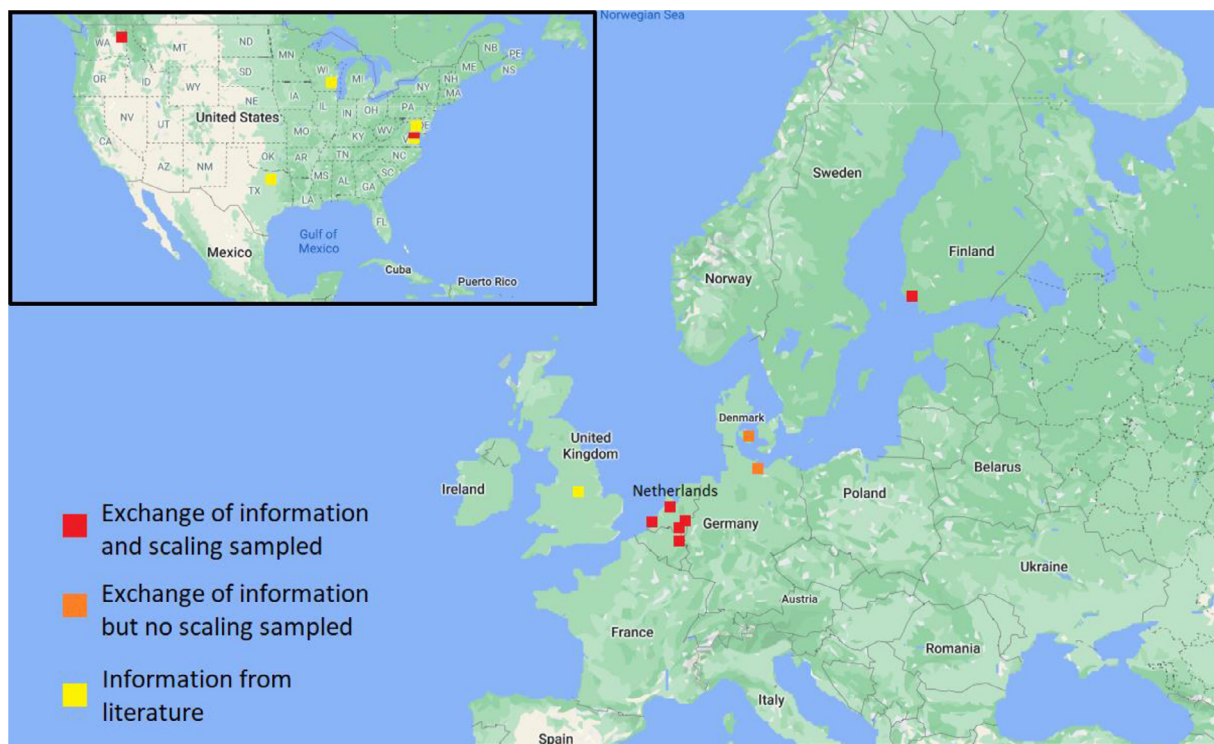
Acknowledgments

Fig. A1. Location of the WWTPs from which data was collected (The Netherlands: 5, USA: 5, Germany: 1, Finland: 1, United Kingdom: 1, Denmark: 1).

Appendix A

Fig. A1

Appendix B

Table B1

Table B1
Equilibrium considered for the modelling with Visual Minteq. The equations and equilibrium constants reported are those used in the database of Visual Minteq.

Equilibrium considered	Log K
$3Fe^{2+} + 2\ PO_4^{3+} + 8H_2O = Fe_3(PO_4)_2 \times 8H_2O$	−35.767
$Fe^{3+} + 3\ H_2O - 3\ H^+ = Fe(OH)_3$	3.2
$PO_4^{3-} + H^+ = HPO_4^{2-}$	12.375
$PO_4^{3-} + 2\ H^+ = H_2PO_4^-$	19.573
$PO_4^{3-} + 3\ H^+ = H_3PO_4$	21.721
$Fe^{2+} + 2\ H_2O - 2\ H^+ = Fe(OH)_2\ (aq)$	−20.494
$Fe^{3+} + 2\ H_2O - 2\ H^+ = Fe(OH)_2^+$	−5.75
$Fe^{2+} + 3\ H_2O - 3\ H^+ = Fe(OH)_3^-$	−30.991
$Fe^{3+} + 3\ H_2O - 3\ H^+ = Fe(OH)_3\ (aq)$	−15
$Fe^{3+} + 4\ H_2O - 4\ H^+ = Fe(OH)_4^-$	−22.7
$Fe^{2+} + H_2O - H^+ = FeOH^+$	−9.397
$Fe^{3+} + H_2O - H^+ = FeOH^{2+}$	−2.02
$2\ Fe^{3+} + 2\ H_2O - 2\ H^+ = Fe_2(OH)_2^{4+}$	−2.894
$3\ Fe^{3+} + 4\ H_2O - 4\ H^+ = Fe_3(OH)_4^{5+}$	−6.288
$Fe^{2+} + 2\ H^+ + PO_4^{3-} = FeH_2PO_4^+$	22.273
$Fe^{3+} + 2\ H^+ + PO_4^{3-} = FeH_2PO_4^{2+}$	23.85
$Fe^{2+} + H^+ + PO_4^{3-} = FeHPO_4\ (aq)$	15.975
$Fe^{3+} + H^+ + PO_4^{3-} = FeHPO_4^+$	22.285

Appendix C

C.1. Power-law parameters determination

To describe the rheology of non-Newtonian fluids like sludge, 3 models are typically used: the Power law model, the Bingham model and the Herschel and Bulkley. Ratkovich et al., 2013 reviewed a number of articles dealing with sludge rheology modelling and concluded that none of these models was better than the others. Moreover, all the 3 models often give a satisfying fitting of the data, which is not surprising since their expression derive one from the other. For this study, the power law model will be used:

$$\tau = K\left(\frac{dv}{dr}\right)^n$$

Where:

- τ is the shear stress in N/m²
- K is the fluid consistency coefficient in N.sⁿ/m²
- $\left(\frac{dv}{dr}\right)$ is the shear rate in s^{-1}
- n is the flow behaviour index (dimensionless)

The constants K and n vary depending on the solid content, temperature and state of digestion of the sludge (Cao et al., 2016). They need to be determined by fitting the experimental data. However, no rheological measurements were done in the current study, so the parameters will be estimated from literature data for sludges with similar properties (TSS=3.1%, $T = 20$ °C, undigested sludge) and modelled with the power law. From the experimental data of Wei et al. (2018), Honey and Pretorius (2020), Füreder et al. (2018) and Rosenberg et al. (2002), we estimate that the parameters will be in the range 0.2–0.4 for n and 2–100 for K (we excluded some much higher K values found in Rosenberg et al. 2002 since it was in contradiction with the 3 other sources).
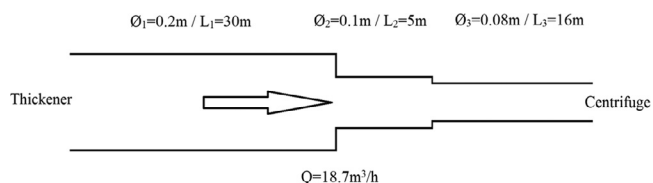
Fig. C1. Piping system where vivianite scaling was found in Hoensbroek WWTP.

C.2. Flow regime evaluation

The piping system in Hoensbroek can be visualized on Fig. C1.

To determine the flow regime in the pipes, the Reynolds number derived from a power law modelling needs to be calculated:

$$Re = \frac{\rho V^{2-n} D^n}{K * 8^{n-1}}$$

Where:

- *Re* is the Reynolds number for the power law model (dimensionless)
- K is the fluid consistency coefficient in $N.s^n/m^2$
- n is the flow behaviour index (dimensionless)
- ρ is the density of the sludge in kg/m^3
- D is the diameter of the pipe in m

Unless it has a very high solid content, sludge has a similar density than water, so is set at $1000 \ kg/m^3$ for the following calculation.

Considering the ranges for the n and K factor estimated above, the Reynolds number in the pipe 3 (d_3=0.08 m / L_3=16 m) varies from 13 to 1679, signifying that the flow regime is laminar since $Re < 2100$ (Ratkovich et al., 2013). This is in line with what is usually reported in literature, where sludge flow in pipes is usually considered laminar (Slatter 2004; Haldenwang et al., 2012). Moreover, the velocity for a laminar/turbulent transition is estimated at 1.5–2.0 m/s (Honey and Pretorius, 2020), while the velocity in the pipe 3 is 1.0 m/s. Considering that pipe 3 is the smallest of the three pipes, a laminar flow should be observed in the 2 other pipes as well (d_1=0.2 m / L_1=30 m and d_2=0.1 m / L_2=5 m).

C.3. Vivianite scaling formation

The authors consider that vivianite scaling could form in 2 ways: by collision of the particles with the pipe wall, and further agglomeration, or by precipitation from the dissolved species following iron reduction in a boundary layer. Considering that the flow regime is laminar in the pipe system, the first formation mechanism is unlikely since it would require some transversal vivianite particle movement. From this point on, the second mechanism is studied.

The pipe 3 at Hoensbroek WWTP has been opened after 3.5 years of operation, and a scaling layer of 0.55 cm had formed. Mössbauer spectroscopy indicates that 72% of the scaling is vivianite. Knowing the density of vivianite (d = 2.69), it means that 39.6 kg of vivianite scaling formed in the pipe 3 over 3.5 years (1.29 g/h).

C.4. Velocity profile in the pipes

From Simpson and Janna (2008) the velocity profile in a circular duct for a non-Newtonian fluid following the power law has the following expression:

$$V_r = \frac{3n+1}{n+1} \left[1 - \left(\frac{r}{R} \right)^{\left(\frac{n+1}{n} \right)} \right] V$$

Where: n is the flow behaviour index (dimensionless) and estimated before ranging on 0.2–0.4

V_r is the velocity at the radius r

r is the distance from the centre of the pipe $(0 < r < R)$

R is the internal radius of the pipe

V is the average velocity in the pipe

For further calculations, n will be fixed at value of 0.3.

C.5. Iron reduction rate

The sludge between the thickener and the centrifuge contains 1070 mg of iron and 560 mg of phosphorus per kg of sludge (TS=3.1%). Under anaerobic conditions, phosphate will be released from the Polyphosphate-Accumulating organisms. However, in chemical sludge (like in Hoensbroek), phosphorus is not only found in PAO's, but is also bound to Fe. Wang et al., 2019 observed that vivianite progressively formed during incubation of activated chemical sludge, meaning that some phosphorus was made available for vivianite formation. It is complicated to differentiate the phosphate released from PAO's and from FeP minerals. Therefore, the estimation of the vivianite scaling formed will be evaluated assuming that iron reduction is the limiting factor.

The quantity of iron reduced can be calculated from the retention time in the different layer of the pipe. According to Wang et al., 2019, iron reduction in sludge in anaerobic conditions is following a first order kinetic with $k = 0.055 \ h^{-1}$. This translates into the reduction of 561 mg of Fe/kg of sludge in the thickener during the residence time of 13.5 h, which will be taken as the initial (Fe_0) value for the subsequent iron reduction. We neglect here the reduction occurring in pipes 1 and 2 due to very low retention time compare to the one in the digester. We obtain the expression:

$$Fe(t) = Fe_0 (1 - \exp(-0.055t))$$

Where:

Fe(t) represents the quantity of iron reduced into Fe2+ after entering the pipe (mg Fe/kg of sludge).

Fe0 is a constant representing the reducible iron at the beginning of the pipe system which is worth 509 of Fe/kg of sludge. (after removing the 561 mg Fe/kg of sludge already reduced in the thickener). t is the time elapsed since the sludge enters pipe (h). It also corresponds to the retention time of the sludge in the pipe at a radius r.

Since the retention times in the pipes are relatively small compared to the iron reduction rate, there is almost a linear relation between the quantity of iron reduced and the retention time. Therefore, the iron reduced is inversely proportional to the velocity of the sludge.

From Fig. C2, it can be noticed that the velocity profile of the sludge in pipe 3 will create zones near the edge of the pipe where Fe^{2+} concentration will be higher, and promote vivianite scaling formation. This iron production in combination with the phosphorus release from the sludge will lead to higher saturation index next to the wall of the pipe than in the bulk (Fig. C3).

C.6. Influence of the pipe diameter on vivianite scaling formation

The evolution of the saturation index (Fig. C3) suggests that the vivianite scaling formation is a wall-mechanism, happening near the edge of the pipe. Therefore, one can assume that bigger pipe would be more favourable than smaller one since their wall area/volume ratio is lower. To confirm this hypothesis, the iron reduction profile was studied for 3 pipes of same length (16 m), and increasing diameter d_1=0.2 m, d_2=0.1 m and d_3=0.08 m. From Fig. C4, it can be seen that a pipe with bigger diameter will logically allow more iron reduction due to an increased sludge retention time.
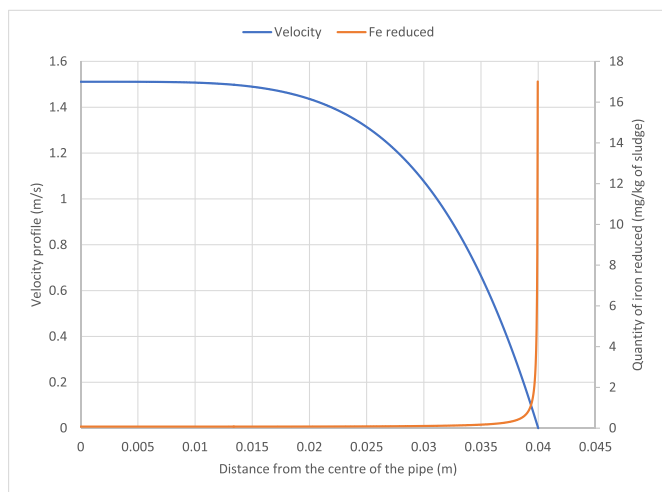
Fig. C2. Left axis: Velocity profile of the sludge in function of its distance from the centre of pipe 3. Right axis: quantity of iron reduced during the stay of the sludge in the pipe in function of its distance to the centre of the pipe.

For further discussion, we arbitrarily assume that vivianite scales in the zones where more than 1 ppm of Fe^{2+} is produced by reduction. From Fig. C4, we can see that this corresponds to a distance to the wall of 13.5, 1.4 and 0.7 mm for pipe of diameter 0.2, 0.1, 0.08 m, respectively. This is explained by the fact that wider pipe will have lower velocity and so bigger retention time, allowing more sludge to be reduced. However, if the sludge has a higher retention time, it also means that the flow will be lower, thus creating less vivianite scaling in terms of weight. For example, there is 7 times more volume of the pipe 1 (d_1=0.2 m) that will have Fe>1 ppm compared to pipe 3 (d_3=0.08 m). However, there will be 43 times more sludge that will effectively be under condition where Fe>1 ppm if the flow in the different sludge layer is taken into account (Table C1). Similar conclusions can be drawn for limit iron concentration other than 1 ppm. From these calculations, and assuming that vivianite scales following a wall mechanism formation, the use of big pipe seems to favour vivianite scaling formation, due to the higher retention time, thus higher iron reduction potential. It is also important to take diffusion into consideration

to verify if the Fe^{2+} atoms have time to reach the wall in their residence time in the pipe.

C.7. Fe^{2+} diffusion

The time that a Fe^{2+} ion will take to reach the wall of the pipe depending on its position can be approximated with the Einstein law of diffusion (Miller 1924):

$$t = \frac{x^2}{2D}$$

Where: t is the time for the particle to cover the distance x (m) x is the distance covered by the particle in the time t (s)

D is the specific diffusion coefficient for the particle studied in the medium considered (m2/s)

Henry 1994 gives the diffusion coefficient of Fe^{2+} in water at 25C: $7,19 \times 10^{-10}$ $m^2.s^{-1}$. Zhang et al., 2016 observed that the diffusion coefficient of Iodide in digested sludge was following a logarithmic relationship to the solid content in the sludge. By extrapolating their data for the solid content of the sludge of Hoensbroek, we can estimate that the diffusion coefficient decreased by 7 times compared to pure water. We estimate that the evolution of the diffusion coefficient will be the same for Fe^{2+} ions, giving $D \sim 10^{-10}$ $m^2.s^{-1}$. Considering the distance to the pipe wall where the quantity of iron reduced is equal to 1 ppm (Table C1), the time required for an atom of Fe^{2+} to diffuse to the wall would be 911,250, 9800 and 2450s for the pipes 1, 2 and 3, respectively. This is much bigger than the retention time of 144 s for the sludge at this location of the pipe. The distance to the pipe wall that would allow Fe^{2+} ions enough time to travel to the pipe wall are 0.28, 0.35 and 0.7 mm for the pipes 1, 2 and 3, respectively. It suggests that even though more Fe^{2+} would be produced in bigger pipes due to higher sludge retention time, a big part of the Fe^{2+} produced would not have time to diffuse to the pipe wall to produce scaling.

To summarize, the morphology of the scaling, and the laminar flow regime suggest that the scaling found in the pipes before dewatering units follow a growth mechanism rather than an agglomeration mechanism. We hypothesize that the iron reduction due to the anaerobic conditions is the driver to the formation of the scaling. The lower sludge residence time in bigger pipes allows more iron to be reduced, potentially creating more scaling.
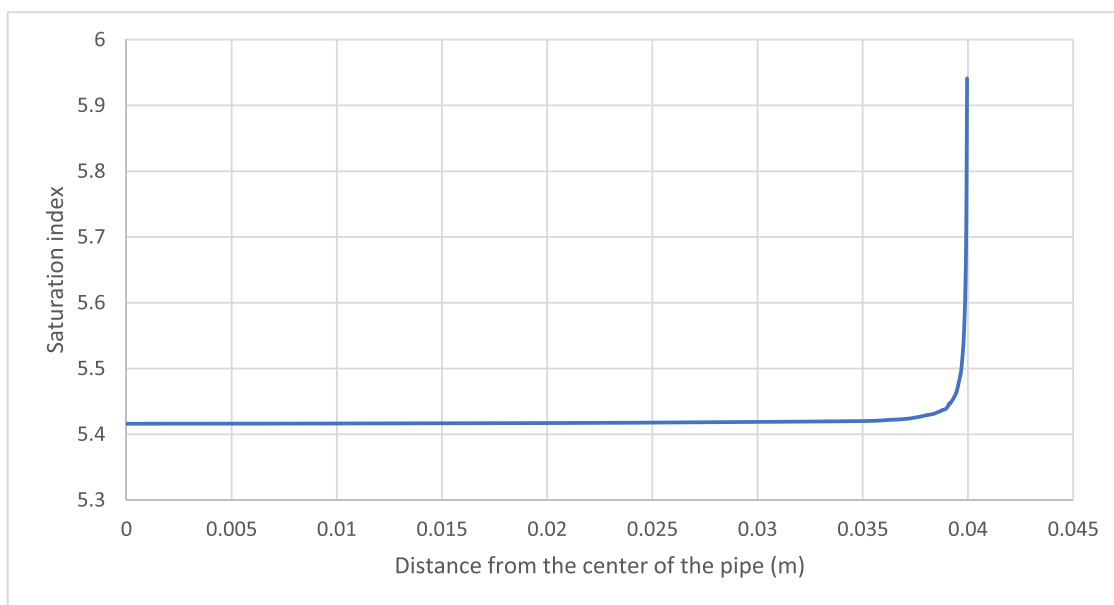
Fig. C3. Saturation index in function of its distance from the centre of pipe 3. The calculation has been realized with Visual Minteq. The input values are taken from a series of measurement in the sludge at the end of pipe 3 (P = 8.6 ppm / Fe^{2+}=27.4 ppm / Fe^{3+}=6.91 ppm / pH=6.9 / SI=0.02).
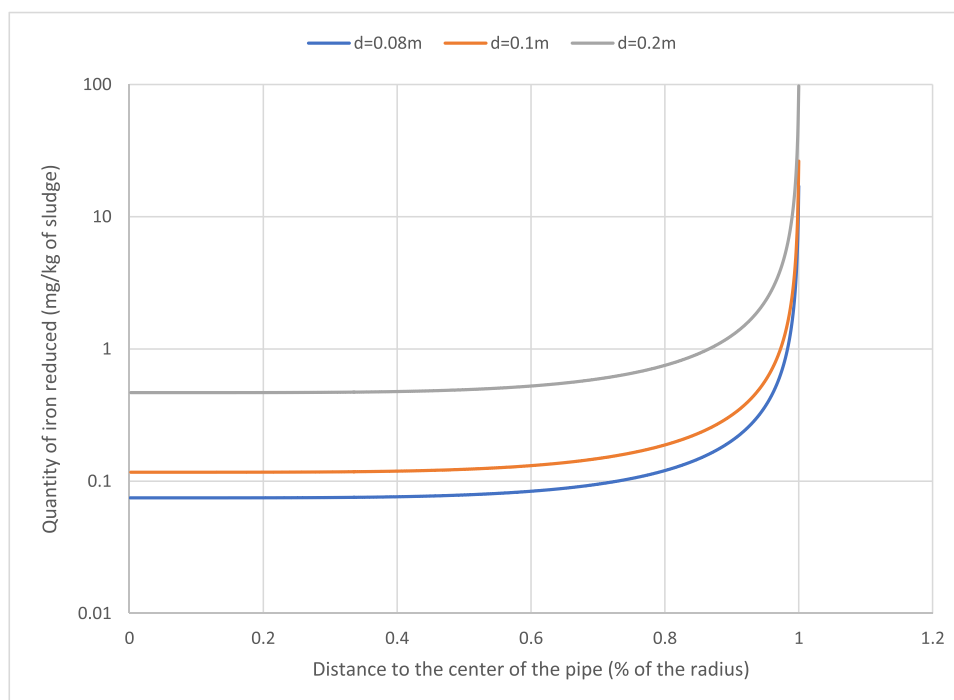
Fig. C4. Quantity of iron reduced in function of the distance to the centre of the pipe for 3 pipes of different diameters ($d = 0.08$, 0.1 and 0.2 m).

Table C1
Characteristics of the pipe section where the quantity of iron reduced is higher than 1 ppm for 3 pipes of different diameter. All pipes considered have a length of 16 m.

Pipe diameter	0.08 m	0.1 m	0.2 m
Distance to the pipe wall where Fe reduction >1ppm	0.7 mm	1.4 mm	13.5 mm
Volume of pipe where Fe reduction >1ppm	3.6%	5.3%	25.2%
Flow of sludge where Fe reduction >1ppm	0.2%	0.5%	9.1%

However, both low diffusion velocity and higher iron concentration near the walls imply that a wall-mechanism growth is possible. These observations imply that bigger pipes may be better to use due to their lower wall area/volume ratio.

According to Wang et al., 2019, iron reduction in sludge in anaerobic conditions is following a first order kinetic with $k = 0.055 \ s^{-1}$. This translates into the reduction of 561 and 1.5 mg of Fe/kg of sludge in the thickener (residence time of 13.5 h) and in the pipe system (residence time of 3.4 min), respectively. Assuming that all the iron reduced in the pipe scales and that 78% of the iron that scales does it as vivianite (data from Mössbauer spectroscopy), 66.0 g of vivianite could form every hour in the pipe system. This translates into the formation of 5.0 g of vivianite per hour in the small pipe section ($\varnothing_3 = 0.08$ m / $L_3 = 16$ m).

When the pipe section before the centrifuge ($d_3 = 0.08$ m) was opened in Hoensbroek, it revealed that the thickness of the scaling was 0.55 cm. The pipe was opened in November 2019, 3.5 years after being installed. Mössbauer spectroscopy indicates that 72% of the scaling is vivianite. Hypothesizing a uniform scaling formation on the entire pipe between the thickener and the centrifuge, and knowing the density of vivianite ($d = 2.69$), 1.39 g/h of vivianite scaling forms. This represents 28% of the value obtained above, which suggests that a significant fraction of the iron reduced stays in the bulk.

Appendix D

The sludge reaching the dewatering units is anaerobic since it has usually been under anaerobic conditions for a couple of hours

(13 h in Hoensbroek for example). Since the solubility of Fe(II) compounds is higher than the one of Fe(III) compounds, the equilibrium concentration of Fe^{2+} is also higher compared to the one of Fe^{3+} as noticed during on-site measurements (Fe^{2+}=27.4 ppm / Fe^{3+}=6.91 ppm before centrifuge in Hoensbroek). During centrifugation, the liquid fraction is separated from the sludge and comes in contact with oxygen so that Fe^{2+} can get oxidized to Fe^{3+}. The freshly formed Fe^{3+} could immediately precipitate due to the lower solubility of Fe(III) compared to Fe(II) compounds. The oxidation of Fe^{2+} is ruled by the following equation:

$$-\frac{d[Fe^{2+}]}{dt} = k[OH^-]^2[Fe^{2+}]P_{O_2}$$

Where:

$[Fe^{2+}]$ is the concentration of Fe^{2+} in mol/L

$[OH^-]$ is the concentration of OH^- in mol/L

P_{O_2} is the partial pressure of O_2 worth 0.2 atm in atmospheric conditions. We assume here that the diffusion of the O_2 is not limiting due to the important mixing. k is the kinetic rate of the reaction in $L^2.mol^{-2}.min^{-1}.atm^{-1}$

According to Sung and Morgan 1980, k is worth $2,9.10^{13}$ $L^2.mol^{-2}.min^{-1}.atm^{-1}$ for an ionic strength of 0.02 M. At a pH of 7.22 (measured in the centrate) and a P_{O_2} of 0.2 (air environment in the centrifuge), 4.1 ppm of Fe^{2+} would be reduced in 1 min, which in the same order of magnitude than the retention time in Hoensbroek centrifuge. It seems like this mechanism would not be too important compared to vivianite formation, which is confirmed by the information collected from the WWTPs: the centrate scaling from Hoensbroek, Blue Plains and Bosscherveld (containing a

Table E1

Evolution of pK_{sp}, SI, P, Fe^{2+} and the vivianite formed at equilibrium for temperature varying from 5 to 90 °C.

Temperature (°C)	pK_{sp}	SI	P at equilibrium (ppm)	Fe^{2+} at equilibrium (ppm)	Vivianite formed at equilibrium (mg/L)
5	35.932	5.586	29.36	13.21	5.35
10	35.870	5.524	29.59	13.84	3.49
15	35.822	5.476	29.77	14.34	1.99
20	35.789	5.443	29.90	14.71	0.87
25	35.767	5.421	29.98	14.93	0.20
30	35.758	5.412	30.02	15.05	−0.14
35	35.760	5.414	30.01	15.02	−0.06
37	35.763	5.417	30.00	15.00	0.00
38	35.766	5.420	29.99	14.95	0.14
40	35.772	5.426	29.97	14.90	0.31
45	35.793	5.447	29.88	14.65	1.06
50	35.824	5.478	29.76	14.32	2.03
55	35.863	5.517	29.61	13.91	3.26
60	35.911	5.565	29.40	13.42	4.72
65	35.966	5.620	29.21	12.89	6.33
70	36.028	5.682	29.00	12.31	8.05
75	36.096	5.750	28.78	11.69	9.91
80	36.171	5.825	28.55	11.05	11.82
85	36.252	5.906	28.31	10.40	13.77
90	36.338	5.992	28.08	9.75	15.71

high quantity of Fe/P species) require regular cleaning, while the one in Turku (mainly iron oxide/hydroxide) needs to be removed only twice a year.

Appendix E

Table E1 Table H1

We consider here a typical digested sludge from a WWTP using CPR with iron. The characteristics of the soluble phase of this sludge at 37 °C are: $P = 30$ ppm, Fe^{2+}=15 ppm, pH=7, IS=0.05 M. Soluble phosphorus, pH and IS are average values obtained from Prot et al., 2020 and Fe^{2+} comes from the results from 4 digested sludge studied by Wilfert et al., 2018.

The software Visual Minteq was used to determine the saturation index and the concentration of the species in func-

tion of the temperature. The value of the pKsp of vivianite was manually modified for each temperature considered following the relation from Al Borno and Tomson 1994: pKsp = −234.205 + 12,242.6/T + 92.510 logT. At 37 °C, the saturation index for vivianite is 5.417. The conditions at 37 °C are considered the equilibrium conditions since it is the usual temperature of digested sludge. All the equilibrium concentrations showed in Table E1 for the different temperatures were calculated to match SI=5.417 as the equilibrium condition.

From the information we collected, the digested sludge is brought typically from 30 °C to 38 °C, which corresponds to a soluble concentration decrease of 0.03 and 0.1 ppm for P and Fe^{2+}, respectively. It corresponds to the formation of 0.28 mg/L of vivianite.

Table H1

Mössbauer spectroscopy parameters for the samples studied. IS=Isomer Shift, QS=Quadrupole Splitting). Fe^{3+}/Fe^{II}: Fe^{3+} species other than vivianite and low-spin Fe^{2+} compounds like pyrite. Fe^{3+}(Viv. $A + B$): total Fe^{3+} vivianite. Fe^{2+}(Viv. A): Fe^{2+} in the site A of vivianite. Fe^{2+}(Viv. B): Fe^{2+} in the site B of vivianite.

Sample	T(K)	IS(mm•s^{-1})	QS(mm•s^{-1})	Phase	Spectral contribution (%)
Anaerobic pipe Hoensbroek	300	0.35	0.81	Fe^{3+}/Fe^{II}	22
		0.47	0.51	Fe^{3+}(Viv. $A + B$)	23
		1.21	2.39	Fe^{2+}(Viv. A)	21
		1.22	2.94	Fe^{2+} (Viv. B)	34
Centrate pipe Hoensbroek	300	0.37	0.77	Fe^{3+}/Fe^{II}	70
		0.47	0.51	Fe^{3+}(Viv. $A + B$)	6
		1.28	2.28	Fe^{2+}(Viv. A)	10
		1.23	2.98	Fe^{2+} (Viv. B)	14
Spokane digester withdrawal	300	0.38	0.79	Fe^{3+}/Fe^{II}	35
		0.47	0.51	Fe^{3+}(Viv. $A + B$)	15
		1.18	2.45	Fe^{2+}(Viv. A)	12
		1.20	2.96	Fe^{2+} (Viv. B)	21
		1.22	1.94	Fe^{2+} (siderite?)	17
Heat Exchanger Amsterdam	300	0.37	0.84	Fe^{3+}/Fe^{II}	32
		0.47	0.51	Fe^{3+}(Viv. $A + B$)	18
		1.24	2.30	Fe^{2+}(Viv. A)	20
		1.20	2.99	Fe^{2+} (Viv. B)	30
Heat Exchanger after THP Blue Plains	300	0.37	0.87	Fe^{3+}/Fe^{II}	25
		0.47	0.51	Fe^{3+}(Viv. $A + B$)	25
		1.22	2.31	Fe^{2+}(Viv. A)	21
		1.20	2.99	Fe^{2+} (Viv. B)	29
Centrate Turku	300	0.37	0.80	Fe^{3+}	100
	4.2	0.43	−0.16	Fe^{3+}(Viv. A)	10
		0.52	−0.18	Fe^{3+}(Viv. B)	13
		0.38	0.02	Ferrihydrite	32
		0.33	0.04	Ferrihydrite	45

Appendix F

Rheological measurements were not carried out with the sludge of Spokane County, so the value of the apparent viscosity of digested sludge was obtained from literature review. The digested sludge of Spokane County has an average solid content of 2–2.5%. Literature indicates that the apparent viscosity of digested sludge ranging from 1.8 to 3.6% of solid varies from 0.035 to 0.5 Pa.s (Markis et al., 2016; Eshtiaghi et al., 2012; Goel et al., 2004, Baudez et al. 2011). These values were taken for shear stresses around 100 s^{-1}. Since sludge is a shear-thinning fluid, its viscosity decreases with increasing shear rate (Markis et al., 2016; Eshtiaghi et al., 2012). In a digester, the shear rates are not homogeneous, and are higher in the zones closer to the stirrer. Baudez et al. 2011, for example show that the apparent viscosity of a 2.5% solid digested sludge decreases from 0.25 to 0.035 Pa.s for an increasing shear rate from 4 to 90 s^{-1}. The shear rate during digestion cannot be too high to preserve the bacteria functioning (Jiang et al., 2016), but high enough to maintain a proper mixing. Therefore, we will consider a case where the shear rate is moderate, and assume a viscosity of 0.1 Pa.s.

Newton's law gives the terminal speed of a particle in sludge:

$$v_{tp} = \sqrt{\frac{4g}{3C_d} * \left(\frac{\rho_p - \rho_s}{\rho_s}\right) * d_p}$$

With:
  v_{tp} the terminal velocity of the particle in m/s
  g is the acceleration of the gravity worth 9.81 m/s2
  C_d is the coefficient of drag
  ρ_p and ρ_s the density of the particle worth 2.7 and 1.0 for vivianite and sludge, respectively
  d_p the diameter of the particle in m
  The coefficient of drag for a sphere is obtained from the Reynolds number through:

$$C_d = \frac{24}{Re} + \frac{3}{\sqrt{Re}} + 0.34$$

Reynolds number for settling particles is:

$$Re = \frac{v_p d_p \rho_v}{\mu}$$

With:
  Re the Reynolds number
  v_p the velocity of the particle in m/s
 d_p the diameter of the particle in m
  μ the apparent viscosity in Pa.s
  Since the flow regime in the digester is most likely laminar, we first hypothesize a *Re* of 1, which gives C_d=27.34, and a terminal velocity of 19 mm/s. By iteration on *Re*, C_d and v_{tp}, we obtain 0.001, 25,000 and 0.63 mm/s, respectively.

For a sludge containing 5% of solid, the viscosity would be around 7–8 times higher than for a sludge containing 2.5% of solids according to Goel et al., 2004 and Baudez et al. 2011. Considering a viscosity of 0.8 Pa.s and following the same iteration principle, we obtain Re=1.5 × 10^{-5}, C_d=1.6 × 10^6 and v_{tp}=0.078 mm/s.

Appendix G
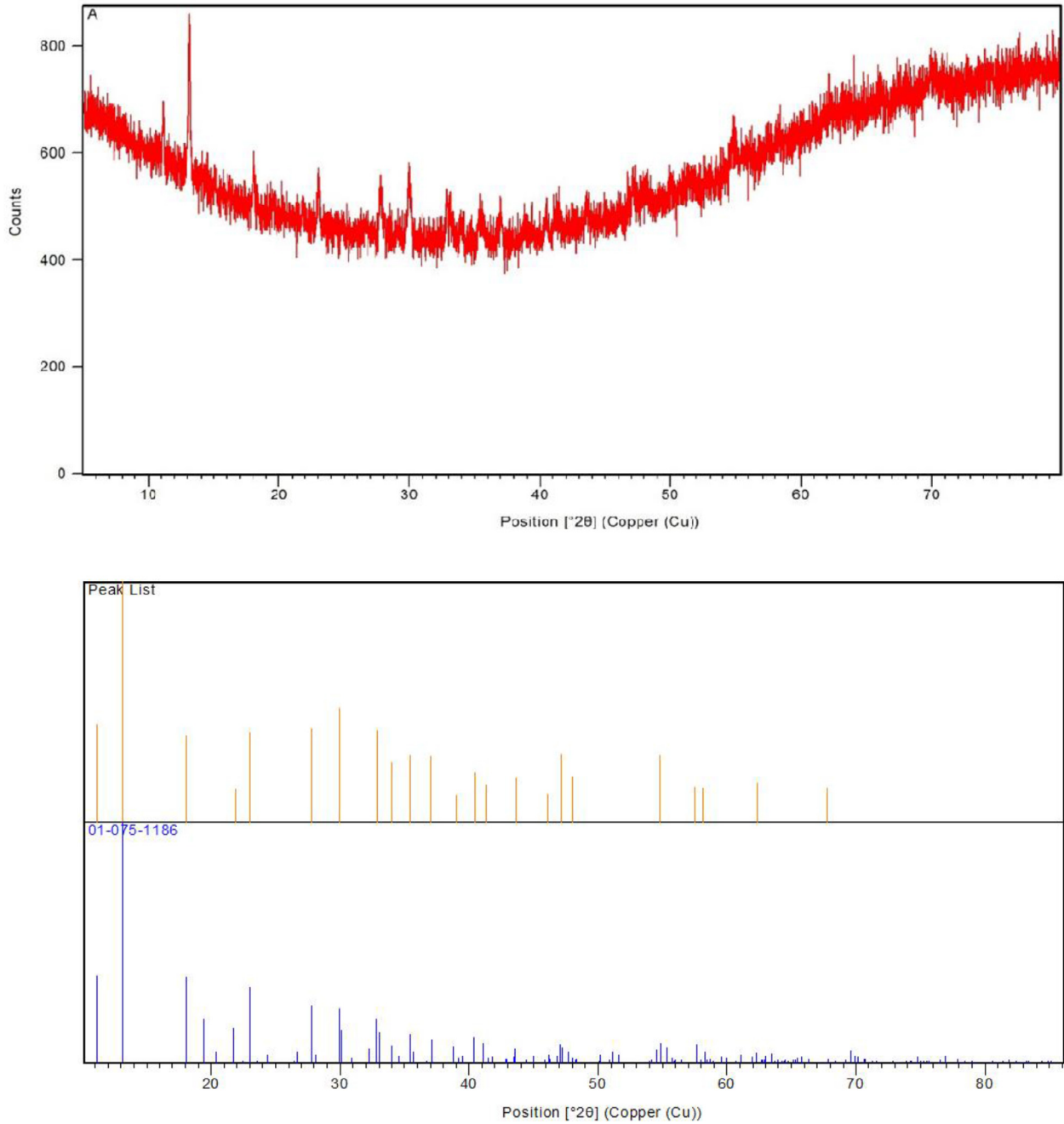
Fig. G1. XRD pattern (top), and plot of identified phases (bottom) for the samples found in the pipes after the thickener in Hoensbroek WWTP. The pattern only revealed the presence of relatively crystalline vivianite.
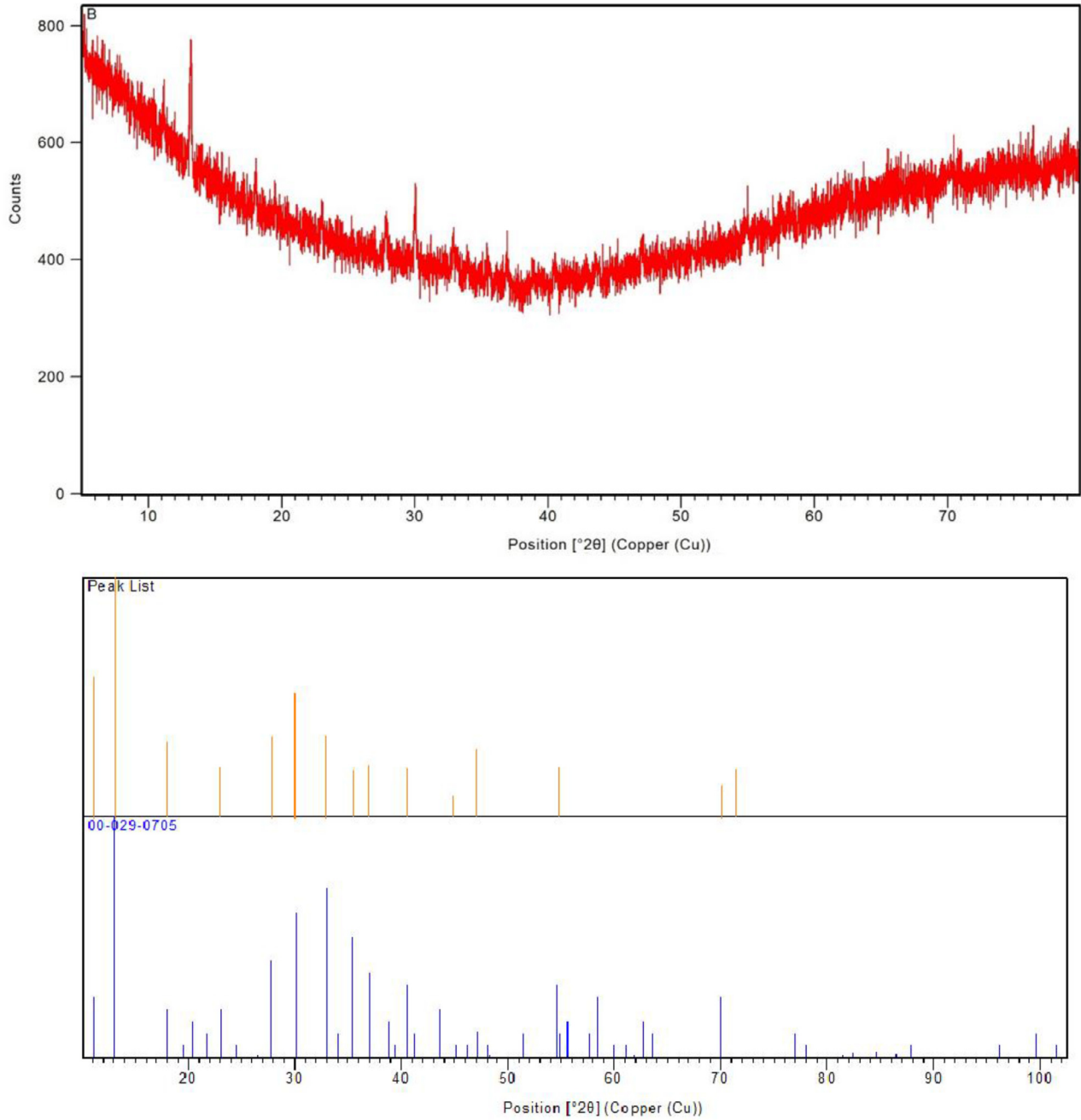
Fig. G2. XRD pattern (top), and plot of identified phases (bottom) of the sample found in the centrate pipe in Hoensbroek WWTP. The pattern only revealed the presence of amorphous material, and impure vivianite.
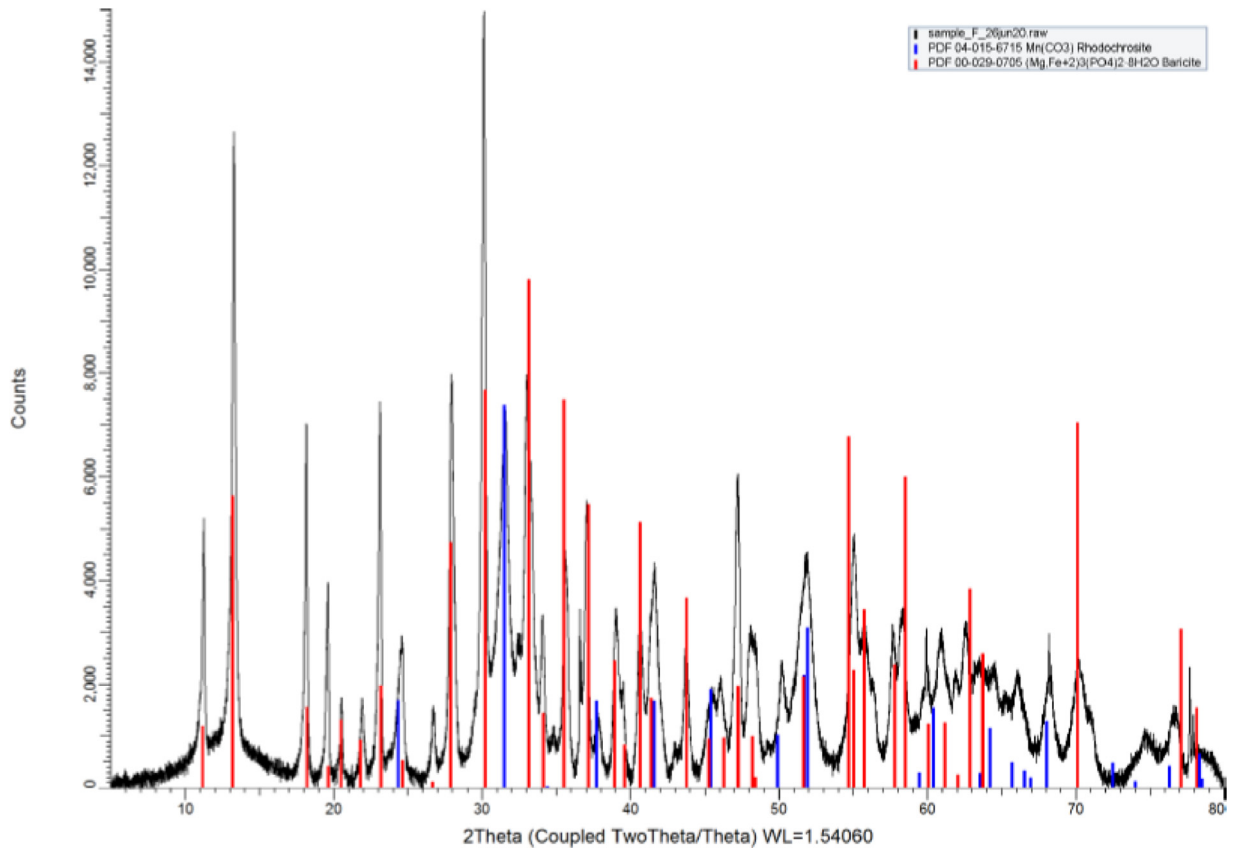
Fig. G3. XRD pattern of the digester withdrawal of Spokane County. The pattern indicates the presence of rhodochrosite (most likely siderite) and baricite (impure vivianite).
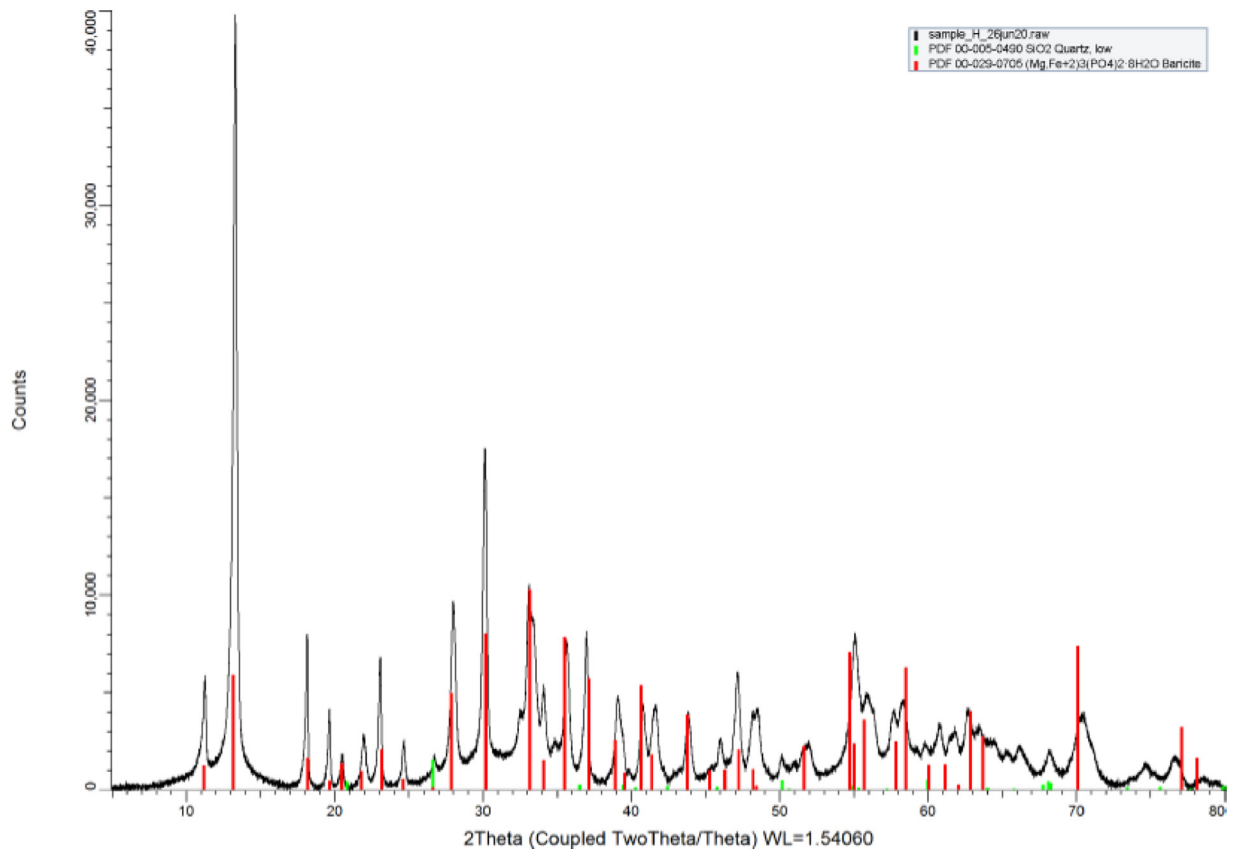

Fig. G4. XRD pattern of the scaling found in the heat exchanger of Amsterdam. The pattern indicates the presence of quartz low and baricite (impure vivianite).
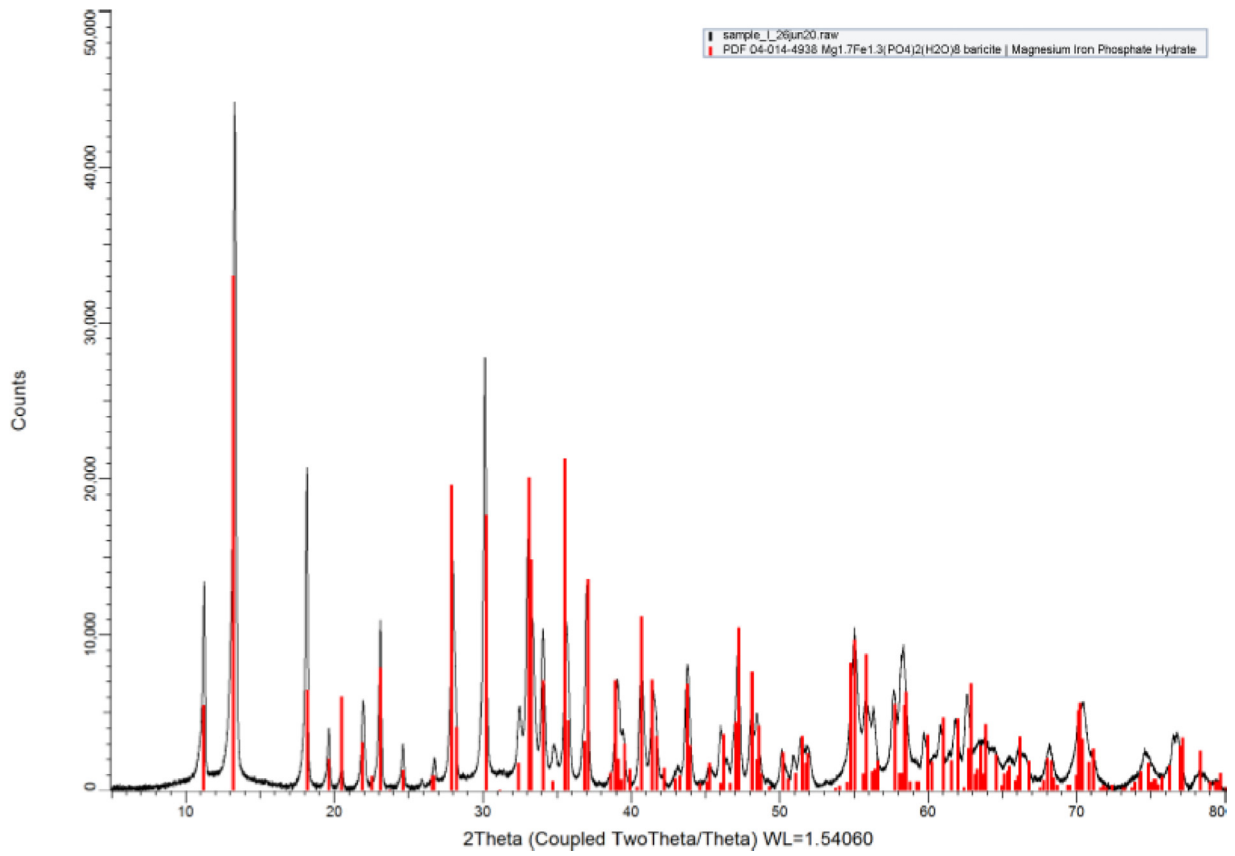
Fig. G5. XRD pattern of the scaling found in the heat exchanger of Blue Plains WWTP after THP. The pattern indicates the presence of baricite (impure vivianite).
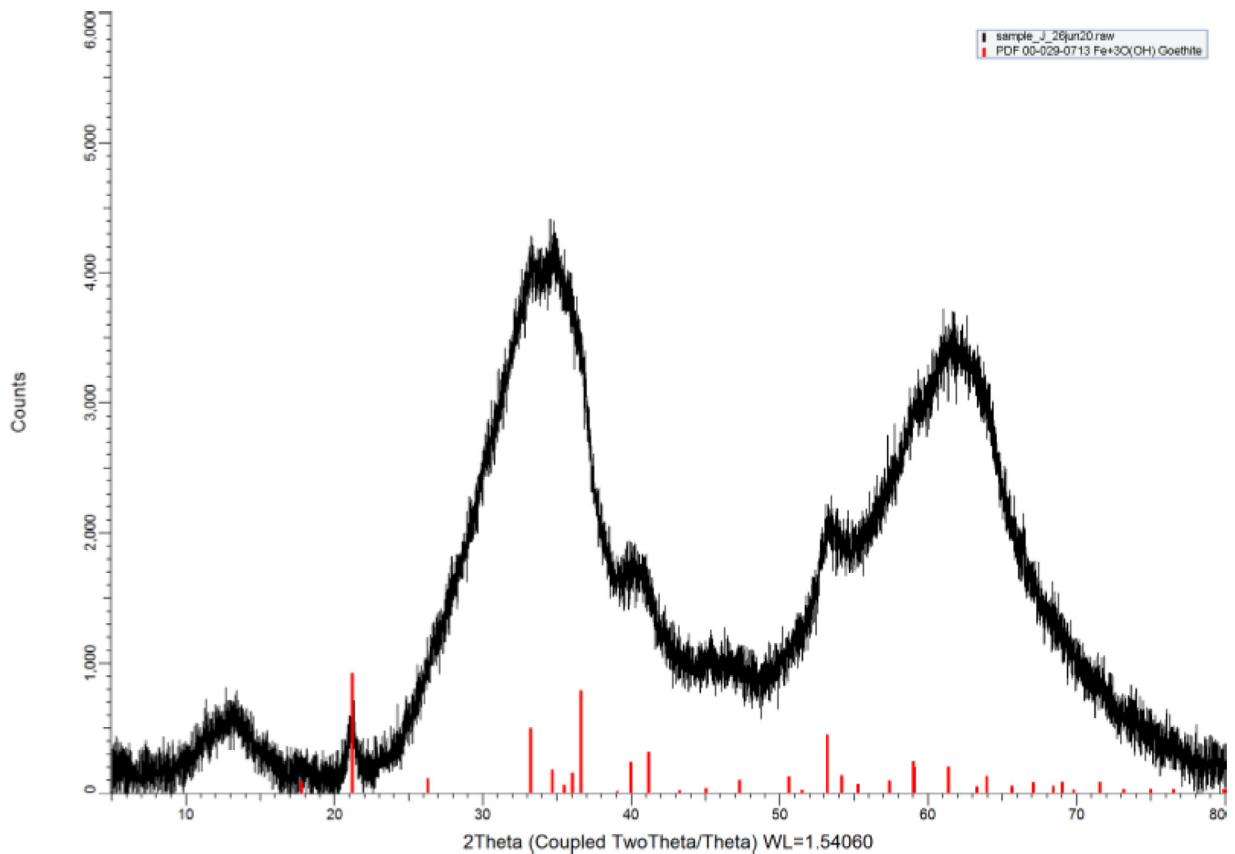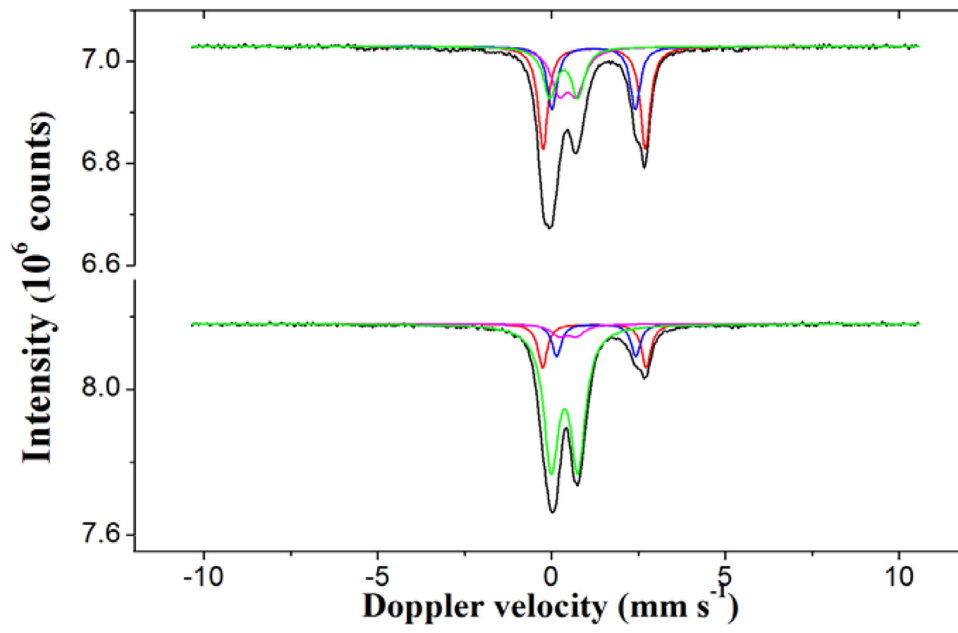

Fig. G6. XRD pattern of the scaling found in the centrate of Turku WWTP. The pattern indicates the presence of amorphous species, with the possible presence of goethite as a minor phase.
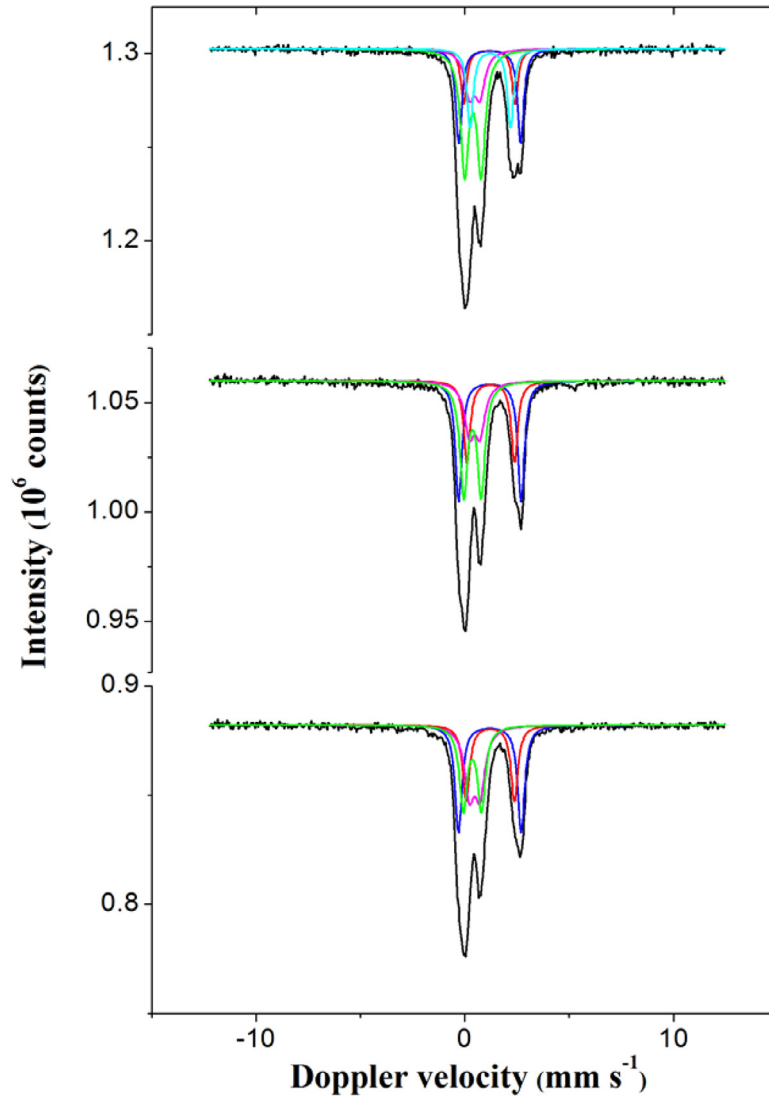
Fig. H1. Mössbauer spectra for the scaling found in the pipe after the thickener (top), and in the centrate pipe (bottom) in Hoensbroek WWTP. Black: total spectrum, Green: Fe^{3+}/Fe^{II}, Pink: Fe3+ (Viv. *A + B*), Blue: Fe^{2+} (Viv. A), Red: Fe^{2+} (Viv. B).

Appendix H

Fig. H2. Mössbauer spectra for the digester withdrawal in Spokane County WWTP (top), the scaling found in the heat exchanger in Amsterdam WWTP (middle), and in the heat exchanger after THP in Blue Plains WWTP (bottom). Black: total spectrum, Green: Fe^{3+}/Fe^{II}, Pink: Fe3+ (Viv. *A + B*), Red: Fe^{2+} (Viv. A), Blue: Fe^{2+} (Viv. B), Cyan: Fe^{2+} (siderite?).

References

Alfa Laval brochure. Last consulted on 17/08/ 2020 at: https://www.alfalaval.com/contentassets/3f718d0f5eeb4d56acc8c7d6eab344a2/alfa_laval_spiral_heat_exchanger_ppi00424en.pdf.

Al-Borno, A., Tomson,, M.B., 1994. The temperature dependence of the solubility product constant of vivianite. Geochim. Cosmochim. Acta 58 (24), 5373–5378. doi:10.1016/0016-7037(94)90236-4.

Battistoni, P., Fava, G., Pavan, P., Musacco, A., Cecchi, F., 1997. Phosphate removal in anaerobic liquors by struvite crystallization without addition of chemicals: preliminary results. *Water Research* 1997 31 (11), 2925–2929. doi:10.1016/S0043-1354(97)00137-1.

Bjorn, A., (2010). Acid Phase Digestion at Derby STW - Context and preliminary optimisation results. Last consulted on 05/11/20 at: https://www.atkinsglobal.com/~/media/Files/A/Atkins-Corporate/group/sectors-documents/water/library-docs/technical-papers/acid-phase-digestion-at-derby.pdf.

Buchanan, A., Chan, T.F., Riches, S., Brookes, A., Brown, C., 2014. Starting up a new advanced digestion technology. 19th European Biosolids & Organic Resources Conference.

Cao, X., Jiang, Z., Cui, W., Wang, Y., Yang, P., 2016. Rheological properties of municipal sewage sludge: dependency on solid concentration and temperature. Procedia Environ. Sci. 31, 113–121. doi:10.1016/j.proenv.2016.02.016.

Čermáková, Z., Švarcová, S., Hradil, D., Bezdicka, P., 2013. Vivianite: a historic blue pigment and its degradation under scrutiny. Sci. Tech. for the Conservation of Cultural Heritage 75–78.

Dormann, J.L., Poullen, J.F., 1980. Étude par spectroscopie Mössbauer de vivianites oxydées naturelles. Bulletin de Minéralogie 103 (6), 633–639. doi:10.3406/bulmi.1980.7431.

Doyle, J., Oldring, K., Churchley, J., Parsons, S., 2002. Struvite formation and the fouling propensity of different materials. Water Res. 36 (16), 3971–3978. doi:10.1016/s0043-1354(02)00127-6.

Doyle, J.D., Parsons, S.A., 2002. Struvite Formation, Control and Recovery. Water Res. 36 (16), 3925–3940. doi:10.1016/S0043-1354(02)00126-4.

El-Bestawy, E., Hussein, H., Baghdadi, H.H., El-Saka, M.F., 2005. Comparison between biological and chemical treatment of wastewater containing nitrogen and phosphorus. J. Ind. Microbiol. Biotechnol. 32 (5), 195–203. doi:10.1007/s10295-005-0229-y.

European commission (2017). Ninth Report on the implementation status and the programs for implementation (as required by Article 17) of council directive 91/271/EEC concerning urban waste water treatment.

Eshtiaghi, N., Markis, F., Slatter, P., 2012. The laminar/turbulent transition in a sludge pipeline. Water Sci. Tech. 65 (4), 697–702. doi:10.2166/wst.2012.893.

European Sustainable Phosphorus Platform. (2019). ESPP wastewater phosphorus removal workshop (133). Last consulted on 06/10/2020 at: https://phosphorusplatform.eu/images/scope/ScopeNewsletter133_Liege_water_policy_workshop_2019.pdf.

Füreder, K., Svardal, K., Krampe, J., Kroiss, H., 2018. Rheology and friction loss of raw and digested sewage sludge with high TSS concentrations: a case study. Water Sci. Tech. (1) 276–286. doi:10.2166/wst.2018.111.

Goel, R., Komatsu, K., Yasui, H., Harada, H., 2004. Process performance and change in sludge characteristics during anaerobic digestion of sewage sludge with ozonation. Water Sci. Tech. 49 (10), 105–113. doi:10.2166/wst.2004.0620.

Guo J.C.Y. Theoretical fluid mechanics: turbulent flow velocity profile, civil engineering, university of colorado at denver. Last consulted on 05/11/2020 at: https://www.ucdenver.edu/faculty-staff/jguo/Documents/Fluid1/12Turbulent.pdf.

Haldenwang, R., Sutherland, A.P.N., Fester, V.G., Holm, R., Chhabra, R.P, 2012. Sludge pipe flow pressure drop prediction using composite power-law friction factor-Reynolds number correlations based on different non-newtonian Reynolds numbers. Water Sa 38 (4), 615–622. doi:10.4314/wsa.v38i4.17.

Henry, V.K., 1994. CRC Handbook of Thermophysical and Thermochemical Data. CRC press Inc, Boca Raton.

Honey, H.C., Pretorius, W.A., 2020. Laminar flow pipe hydraulics of pseudoplastic-thixotropic sewage sludges. Water Sa 26 (1).

Janssen, P.M.J., Meinema, K., van de Roest, H.F, 2002. Biological Phosphorus Removal, Manual for Design and Operation.

Jiang, J., Wu, J., Poncin, S., Li, H.Z., 2016. Effect of hydrodynamic shear on biogas production and granule characteristics in a continuous stirred tank reactor. Proc. Biochem. 51 (3), 345–351. doi:10.1016/j.procbio.2015.12.014.

Klencsár, Z., 1997. Mössbauer spectrum analysis by Evolution Algorithm. Nuclear Instruments and Methods in Physics Research Section B: Beam Interactions with Materials and Atoms 129 (4), 527–533. doi:10.1016/s0168-583x(97)00314-5.

Kumar, P.S., Korving, L., Van Loosdrecht, M.C.M., Witkamp, G.J, 2018. Adsorption as a technology to achieve ultra-low concentrations of phosphate: research gaps and economic analysis. Water Research X 4. doi:10.1016/j.wroa.2019.100029.

Kumar, P.S., Korving, L., Keesman, K.J., van Loosdrecht, M.C.M., Witkamp, G.J., 2019. Effect of pore size distribution and particle size of porous metal oxides on phosphate adsorption capacity and kinetics. Chem. Eng. J. 358. doi:10.1016/j.cej.2018.09.202.

Lines, J.R. (1991). Heat Exchangers in municipal wastewater treatment plants. Last consulted on 29/10/2020 at: https://www.graham-mfg.com/usr/pdf/TechLibHeatTransfer/13.PDF.

Liu, J., Cheng, X., Qi, X., Li, N., Tian, J., Qiu, B., Qu, D., 2018. Recovery of phosphate from aqueous solutions via vivianite crystallization: thermodynamics and influence of pH. Chem. Eng. J. 349, 37–46. doi:10.1016/j.cej.2018.05.064.

Markis, F., Baudez, J.-C., Parthasarathy, R., Slatter, P., Eshtiaghi, N., 2016. Predicting the apparent viscosity and yield stress of mixtures of primary, secondary

and anaerobically digested sewage sludge: simulating anaerobic digesters. Water Res. 100, 568–579. doi:10.1016/j.watres.2016.05.045.

Marx, J.J., Wilson, T.E., Schroedel, R.B., Winfield, G., Sokhey, A., 2001. Vivianite: nutrient's removal hidden problem. Proceedings of the Water Environment Federation 8, 378–388. doi:10.2175/193864701790861721.

McCammon, C.A., Burns, R.G., 1980. The oxidation mechanism of vivianite as studied by mossbauer spectroscopy. Am. Mineral. 65 (3–4), 361–366.

Medina, G., Tabares, J.A., Pérez Alcázar, G.A., Barraza, J.M., 2006. A methodology to evaluate coal ash content using siderite mössbauer spectral area. Fuel 85 (5–6), 871–872. doi:10.1016/j.fuel.2005.08.034.

Meroney, R.N., Colorado, P.E., 2009. CFD simulation of mechanical draft tube mixing in anaerobic digester tanks. Water Res. 43 (4), 1040–1050. doi:10.1016/j.watres.2008.11.035.

Mersmann, A., 2001. Crystallization Technology handbook, Second edition Revised and Explained.

Miller, C.C., 1924. The Stokes-Einstein law for diffusion in solution. Proceedings of the Royal Soc. London. Series a, Containing Papers of a Mathematical and Physical Character 106 (740), 724–749.

Panter, K., Holte, H., Walley, P. (2013). Challenges of developing small scale thermal hydrolysis and digestion projects. *18th European Biosolids & Organic Resources Conference & Exhibition*.

Partlan, E., (2018). BlueTech Report on LIFT Water Technology Survey: wastewater. Last consulted on 29/10/2020 at: https://www.waterrf.org/sites/default/files/file/2019-07/LIFT%20Water%20Technology%20Survey%20Report%20-%20Wastewater_0.pdf.

Pathak, B., Al-Omari, A., Smith, S., Passarelli, N., Suzuki, R., Khakar, S., DeBarbadillo, C., 2018. Vivianite occurrence and remediation techniques in biosolids pre-treatment process. WEF Residuals and Biosolids Conference 2018.

Pratesi, G., Cipriani, C., Giuli, G., Birch, W., 2003. Santabarbaraite: a new amorphous phosphate mineral. Eur. J. Mineral. 15 (1), 185–192. doi:10.1127/0935-1221/2003/0015-0185.

Priambodo, R., Tan, P.R., Shih, Y.-.L., Huang, Y.-.J., 2017. Fluidized-bed crystallization of iron phosphate from solution containing phosphorus. J.. Taiwan Inst. Chem. Engrs. 80, 247–254. doi:10.1016/j.jtice.2017.07.004.

Prot, T., Nguyen, V.H., Wilfert, P., Dugulan, A.I., Goubitz, K., De Ridder, D.J., Korving, L., Rem, P., Bouderbala, A., Witkamp, G.J., Van Loosdrecht, M.C.M., 2019. Magnetic separation and characterization of vivianite from digested sewage sludge. Separation and Purification doi:10.1016/j.seppur.2019.05.057.

Prot, T., Wijdeveld, W., Eshun, L.E., Dugulan, A.I., Goubitz, K., Korving, L., Van Loosdrecht, M.C.M, 2020. Full-Scale Increased Iron Dosage to Stimulate the Formation of Vivianite and Its Recovery from Digested Sewage Sludge. Water Res. 182. doi:10.1016/j.watres.2020.115911.

Ratkovich, N., Horn, W., Helmus, F.P., Rosenberger, S., Naessens, W., Nopens, I., Bentzen, T.R., 2013. Activated sludge rheology: a critical review on data collection and modelling. Water Res. 47 (2), 463–482. doi:10.1016/j.watres.2012.11.021.

Rawn, A.M., Banta, A.P., Pomeroy, R., 1939. Multiple stage sewage digestion. Am. Soc. Civil Engr. Trans. 105, 93–132.

Refait, P.H., Abdelmoula, M., Génin, J.-M.R., 1998. Mechanisms of formation and structure of green rust one in aqueous corrosion of iron in the presence of chloride ions. Corros. Sci. 40 (9), 1547–1560. doi:10.1016/S0010-938X(98)00066-3.

Reusser, S.R., 2009. Proceed with caution in advanced anaerobic digestion system design. Proceedings of the Water Environment Federation Session 41 (50), 3065–3084.

Roldán, R., Barrón, V., Torrent, J., 2002. Experimental alteration of vivianite to lepidocrocite in a calcareous medium. Clay Miner 37 (4), 709–718. doi:10.1180/0009855023740072.

Rosenberger, R., Kubin, K., Kraume, M., 2002. Rheology of activated sludge in membrane bioreactors. Eng. Life Sci. 2 (9), 269–275. doi:10.1002/1618-2863(20020910)2, 9<269::aid-elsc269>3.0.co;2-v.

Rothe, M., Kleeberg, A., Hupfer, M., 2016. The occurrence, identification and environmental relevance of vivianite in waterlogged soils and aquatic sediments. Earth-Sci. Reviews 158, 51–64. doi:10.1016/j.earscirev.2016.04.008.

Salehin, S., Kulandaivelu, J., Rebosura Jr., M, Khan, W., Wong, R., Jiang, G., Smith, P., McPhee, P., Howard, C., Sharma, K., Keller, J., Donose, B.C., Yuan, Z., Pikaar, I., 2019. Opportunities for reducing coagulants usage in urban water management: the Oxley Creek sewage collection and treatment system as an example. Water Res. 165. doi:10.1016/j.watres.2019.114996, 114996–114996.

Schwertmann, U. (1991). Solubility and dissolution of iron oxides. *Iron Nutrition and Interactions in Plants*,3–27. doi:10.1007/978-94-011-3294-7_1.

Seitz, A., Riedner, J., Malhotra, K., Kipp, J., 1973. Iron-Phosphate compound identification in sewage sludge residue. Environ. Sci. Technol. 7 (4), 354–357. doi:10.1021/es60076a005.

Shimada, T., Evers, M., White, J., Kaakaty, C., Sober, J., Kilian, R., 2011. Detection and mitigation of vivianite scaling in anaerobic digesters. Weftec 2011.

Simpson, M.M., Janna, W. (2008). Newtonian and non-newtonian fluids: velocity profiles, viscosity data, and laminar flow friction factor equations for flow in a circular duct conference. *ASME 2008 International Mechanical Engineering Congress and Exposition*. doi:10.1115/IMECE2008-67611.

Slatter, P., 2004. The hydraulic transportation of thickened sludges. Water S.A 30 (5). doi:10.4314/wsa.v30i5.5169.

Solon, K., Volcke, E.I.P., Spérandio, M., van Loosdrecht, M.C.M, 2019. Resource recovery and wastewater treatment modelling. Environ. Sci: Water Res. Tech. (4) doi:10.1039/c8ew00765a.

Spiralex brochure. Last consulted on 17/08/2020 at https://www.spiralex.nl/wp-content/uploads/2017/08/Sludge.pdf.</bib

Sung, W., Morgan, J.J., 1980. Kinetics and product of ferrous iron oxygenation in aqueous systems. Environ. Sci. Technol. 14 (5), 561–568. doi:10.1021/es60165a006.

Wang, R., Wilfert, P., Dugulan, I., Goubitz, K., Korving, L., Witkamp, G.-J., van Loosdrecht, M.C.M., 2019. Fe(III) reduction and vivianite formation in activated sludge. Sep Purif. Technol. 220, 126–135. doi:10.1016/j.seppur.2019.03.024.

Wilfert, P., Kumar, P.S., Korving, L., Witkamp, G.-J., van Loosdrecht, M.C.M., 2015. The relevance of phosphorus and iron chemistry to the recovery of phosphorus from wastewater: a review. Environ. Sci. Technol. 49 (16), 9400–9414. doi:10.1021/acs.est.5b00150.

Wilfert, P., Mandalidis, A., Dugulan, A.I., Goubitz, K., Korving, L., Temmink, H., Witkamp, G.J., van Loosdrecht, M.C.M., 2016. Vivianite as an important iron phosphate precipitate in sewage treatment plants. Water Res. 104, 449–460. doi:10.1016/j.watres.2016.08.032.

Wilfert, P., Korving, L., Dugulan, I., Goubitz, K., Witkamp, G.J., van Loosdrecht, M.C.M., 2018. Vivianite as the main phosphate mineral in digested sewage sludge and its role for phosphate recovery. Water Res. 144, 312–321. doi:10.1016/j.watres.2018.07.020.

Yousuf, M., Frawley, P.J., 2018. Experimental evaluation of fluid shear stress impact on secondary nucleation in a solution crystallization of paracetamol. Cryst Growth Des doi:10.1021/acs.cgd.8b01074.

Wei, P., Tan, Q., Uijttewaal, W.S.J., van Lier, J.B., de Kreuk, M.K, 2018. Experimental and mathematical characterisation of the rheological instability of concentrated waste activated sludge subject to anaerobic digestion. Chem. Eng. J. 349. doi:10.1016/j.cej.2018.04.108.

Zhang, Y., Li, H., Cheng, Y., Liu, C., 2016. Influence of solids concentration on diffusion behavior in sewage sludge and its digestate. Chem. Eng. Sci. 152, 674–677. doi:10.1016/j.ces.2016.06.058.